Aridity weakens population-level effects of multiple species interactions on *Hibiscus meyeri*

Allison M. Louthan[a,b,c,1], Robert M. Pringle[b,d], Jacob R. Goheen[b,e], Todd M. Palmer[b,f], William F. Morris[a], and Daniel F. Doak[b,c]

[a]Department of Biology, Duke University, Durham, NC 27708; [b]Mpala Research Centre, Nanyuki 10400, Kenya; [c]Environmental Studies Program, University of Colorado, Boulder, CO 80309; [d]Department of Ecology and Evolutionary Biology, Princeton University, Princeton, NJ 08544; [e]Program in Ecology, Department of Zoology and Physiology, University of Wyoming, Laramie, WY 82071; and [f]Department of Biology, University of Florida, Gainesville, FL 32611

Edited by Hugh P. Possingham, University of Queensland, St. Lucia, QLD, Australia, and approved November 14, 2017 (received for review May 22, 2017)

Predicting how species' abundances and ranges will shift in response to climate change requires a mechanistic understanding of how multiple factors interact to limit population growth. Both abiotic stress and species interactions can limit populations and potentially set range boundaries, but we have a poor understanding of when and where each is most critical. A commonly cited hypothesis, first proposed by Darwin, posits that abiotic factors (e.g., temperature, precipitation) are stronger determinants of range boundaries in apparently abiotically stressful areas ("stress" indicates abiotic factors that reduce population growth), including desert, polar, or high-elevation environments, whereas species interactions (e.g., herbivory, competition) play a stronger role in apparently less stressful environments. We tested a core tenet of this hypothesis—that population growth rate is more strongly affected by species interactions in less stressful areas—using experimental manipulations of species interactions affecting a common herbaceous plant, *Hibiscus meyeri* (Malvaceae), across an aridity gradient in a semiarid African savanna. Population growth was more strongly affected by four distinct species interactions (competition with herbaceous and shrubby neighbors, herbivory, and pollination) in less stressful mesic areas than in more stressful arid sites. However, contrary to common assumptions, this effect did not arise because of greater density or diversity of interacting species in less stressful areas, but rather because aridity reduced sensitivity of population growth to these interactions. Our work supports classic predictions about the relative strength of factors regulating population growth across stress gradients, but suggests that this pattern results from a previously unappreciated mechanism that may apply to many species worldwide.

abiotic stress | climate change | population growth | range boundaries | species interactions

Understanding the relative strength of the factors that regulate population growth and abundance is a fundamental goal of ecology. In the era of anthropogenic climate change, it is particularly important to understand what factors allow populations to persist and set species' range boundaries (1–4). Although we know that climate and other abiotic factors can constrain geographic ranges (2), theoretical and empirical studies show that predation, competition, and other species interactions can also limit population growth substantially enough to set range boundaries (5–8). One long-standing hypothesis, first proposed by Darwin (5), predicts that abiotic factors should set range boundaries in areas that are cold, dry, or both (hereafter "stressful environments"), whereas species interactions should set boundaries in less stressful environments. We refer to this idea, which has been discussed by multiple authors since Darwin (6–8) but never clearly named, as the species interactions–abiotic stress hypothesis (SIASH). Here, we use changes in estimated population growth rate as a metric of species interactions' effect size ("intensity" sensu ref. 9), and, as in previous work (8), we define "stress" as any abiotic condition, including but not limited to resource limitation, that reduces mean fitness or population growth rate. There are numerous experimental tests of this idea, but most focus on single interactions (e.g., refs. 10 and 11) and on small-scale gradients; most notably, antagonistic interactions across intertidal depths have generally supported the hypothesis (12, 13). Correlative data, such as abundance records (ref. 14, although see refs. 15 and 16) and studies of species distribution models (17) suggest that it might manifest across broader spatial scales (18, 19); patterns of cosympatry also provide mixed support (20, 21).

Nonetheless, we still require large-scale experimental tests of the generality of SIASH, tests of the mechanisms generating differential effects of species interactions across stress gradients, and simultaneous consideration of multiple types of species interactions (8). Opposing effects of different species interactions, multiple interacting stress gradients, or range boundaries caused by other factors (such as dispersal limitation, lack of genetic variability in peripheral populations, or other nondemographic constraints) could all limit the generality of Darwin's conjecture. In fact, the stress gradient hypothesis, which enjoys considerable empirical support, predicts that the intensity of positive vs. negative effects (but not necessarily net effect size) of species interactions should vary systematically with stress (22). While there is some evidence that both negative and positive interactions should set similar range limits (23), Darwin predicted only how the strength of antagonistic interactions varies across stress gradients (5). Despite this mixed empirical and theoretical support,

Significance

Predicting the impacts of global change on biodiversity requires understanding the factors that regulate population growth and set species' range boundaries. Darwin proposed that abiotic factors limit population growth in stressful areas, whereas species interactions dominate in less stressful environments because of an increased density and diversity of enemies (consumers, parasites, pathogens). We present experimental support for this hypothesized shift in the strength of species interactions with climate, but we also show that this pattern does not arise from Darwin's proposed mechanism. Our work implies that effects of species interactions on population growth rate decrease with stress, with implications for how different range boundaries are likely to respond to climatic change.

Author contributions: A.M.L. and D.F.D. designed research; A.M.L., R.M.P., J.R.G., T.M.P., W.F.M., and D.F.D. performed research; A.M.L. analyzed data; and A.M.L., R.M.P., J.R.G., T.M.P., W.F.M., and D.F.D. wrote the paper.

The authors declare no conflict of interest.

This article is a PNAS Direct Submission.

Data deposition: The data used to construct integral projection models and project population growth rates, as well as the data used in the *Supporting Information*, have been deposited in figshare (https://doi.org/10.6084/m9.figshare.5660608.v2).

[1]To whom correspondence should be addressed. Email: allisonmlouthan@gmail.com.

This article contains supporting information online at www.pnas.org/lookup/suppl/doi:10.1073/pnas.1708436115/-/DCSupplemental.

SIASH has recently been invoked to explain broad-scale patterns in species' abundance and distribution, including discrepancies between trailing and leading range boundary dynamics (19, 24).

The central premise of SIASH is that species interactions strongly limit population growth rate in less stressful areas, ultimately driving populations into decline, but have little effect on population growth rate in more stressful areas (8). Darwin originally proposed—and it is still commonly assumed—that higher densities or diversities of interacting species in less stressful areas generate stronger population-level effects of species interactions (5, 7, 25); we call this the "density mechanism." However, at least two other mechanisms could also generate this pattern. The "per capita impact mechanism" predicts that each individual interactor exerts stronger effects on vital rates (e.g., survival, growth, and reproduction) in less stressful areas. For example, an herbivore could consume more plant tissue in mesic areas because plants are more palatable or occur at higher densities, making them easier to find. The "life history mechanism" could operate if stress alters species' demographic patterns such that the same per capita effects and interactor densities generate stronger effects on population growth in less stressful areas. For example, if offspring establishment is higher in less stressful areas, then population growth may be more sensitive to herbivore-induced reductions in plant reproductive output in these areas than in more stressful sites.

Here, we experimentally test how multiple types of species interactions impact population growth rate across an abiotic stress gradient, and how differences in interaction strengths arise. We quantified the effects of four species interactions, including both positive and negative interaction types, on vital rates and population growth rates of a common African plant, *Hibiscus meyeri* (Malvaceae), across an aridity gradient in central Kenya. *H. meyeri* occurs in semiarid savannas, where plants experience (*i*) water limitation; (*ii*) both competitive and facilitative effects from neighboring shrubby and herbaceous plants (26); (*iii*) browsing by a diverse array of large mammals (27); and (*iv*) variability in insect-mediated outcross pollination (*Supporting Information*).

Results

At three sites across the stress gradient (Arid, Intermediate, and Mesic, collectively spanning a 22% increase in mean annual precipitation; ref. 28), we collected demographic data over 4 y on *H. meyeri* plants that varied in their distance to woody plants ("shrubs"), and that were subjected to factorial manipulation of (*i*) mammalian herbivores (27) (Fig. S1) and (*ii*) neighboring (<30-cm) herbaceous vegetation. We estimated effects of rainfall in the year before measurement, neighboring herbaceous plant cover ("herbs"), distance to nearest shrub, and herbivory ("herbivores," as estimated by the amount of mammalian herbivore dung) on five classes of vital rates (size-specific survival, growth, probability of fruiting, number of fruits given fruiting, and fruit-to-seedling transition rate), using mixed models with block as a random effect (Fig. S1). To simulate the positive effects of pollinator presence, we increased predicted values of seeds per fruit and fruits per plant (the two vital rates affected by inbreeding depression in a congener; ref. 29 and *Supporting Information*), as pollinators alleviate the inbreeding depression associated with facultative self-pollination (30), the most common type of pollination for *H. meyeri*. Species interactions and aridity influenced multiple vital rates, with the strongest aridity effects on fruit-to-seedling transition rate and strongest species interaction effects on decrease in reproduction due to shrub proximity and herbivore presence (Fig. S2 and Table S1).

We combined vital rate estimates to estimate stochastic population growth rate (λ_s) as functions of both stress (i.e., temporal and spatial variation in rainfall) and each type of species interaction using integral projection models (IPMs) (31), which, like other demographic models, use size- or other stage-specific estimates of different vital rates to generate estimates of population growth. We then simulated removal of herbs, shrubs, or mammalian herbivores (by reducing interactor densities to approximately zero in our mixed models and recalculating λ_s; *Supporting Information*) or addition of pollinators (by increasing predicted values of seeds per fruit and fruits per plant, as described above; hereafter, "simulated pollinators") to quantify the effect of each interaction on λ_s at each site. We then asked whether the strength of these effects differed consistently from the Mesic to Arid site (Fig. 1 and Fig. S3).

Effects of aridity and species interactions on population growth rate were all in the predicted directions: Arid λ_s was lower than Mesic λ_s, and the removal of consumptive or net competitive effects (i.e., herbs, shrubs, and herbivores) or addition of positive interactions (simulated pollinators), increased λ_s at all three sites (Fig. 1). The magnitudes of effects of all four species interactions were also consistent with SIASH's predictions: effects of each interaction on λ_s increased from the Arid to the Mesic site (Fig. 1). This consistent effect was observed even for simulated pollinators, a positive species interaction, and even when a species interaction had positive effects on one vital rate(s) and negative effects on others (e.g., removing shrubs reduced survival but increased number of fruits among plants that fruited; Fig. S2 and Table S1). Support for SIASH was also robust to model and parameter uncertainty, which we quantified by estimating a relative interaction effect (RIE) index, the difference between ln[(λ_s with herb, shrub, or herbivore removal, or simulated pollinator addition)/(λ_s under field conditions)] at the Mesic vs. Arid site for 1,000 sets of random vital rate models and parameter values (Fig. 2 and Fig. S3). RIE values, which compare the effect of a species interaction on λ_s between our two climatically extreme sites, were consistently greater than zero, conforming to SIASH predictions.

To test how the density, per capita impact, and life history mechanisms each contributed to stronger effects of species interactions on population growth under less stressful conditions, we decomposed RIE values into the relative contribution of each mechanism by reestimating RIE while holding the various parameters controlling nontarget mechanisms constant in the underlying vital rate functions (*Materials and Methods*). For shrubs, herbivores, and simulated pollinators, the life history mechanism almost entirely accounted for stronger effects in the Mesic site (Fig. 3). For *H. meyeri*'s interaction with herbs, the density mechanism also contributed substantially to stronger effects in the Mesic site. For herbivory, the density mechanism actually reduced RIE values due to higher herbivore activity at the Arid site during our study (28) (*Supporting Information*).

The strong support for the life history mechanism means that population growth was more sensitive at the Mesic than the Arid site to changes in one or more vital rates that were influenced by each species interaction. To isolate the contribution of each vital rate's variation with aridity to the difference in effects of species interactions across sites, we adopted a similar approach to that described for our first decomposition. In these RIE calculations, λ_s estimates were generated using site-specific values of the target species interaction on all vital rates, but values of only the target vital rate included site-specific rainfall and block effects (*Materials and Methods*), isolating the effects of aridity-driven vital rate differences.

For each species interaction, changes across sites in a single vital rate generated the majority of the SIASH pattern. For interactions with herbs, shrubs, and simulated pollinators, changes in the fruit-to-seedling transition rate (Fig. S2) generated essentially the entire pattern of stronger effects of species interactions at the Mesic site (Fig. 4). For herbs and simulated pollinators, these effects were at least partially direct, as these species interactions affected fruit-to-seedling transition rate (Fig. S2 and Table S1). By contrast, for shrubs, these effects were entirely indirect: shrubs did not directly affect fruit-to-seedling transition rate (Fig. S2 and Table

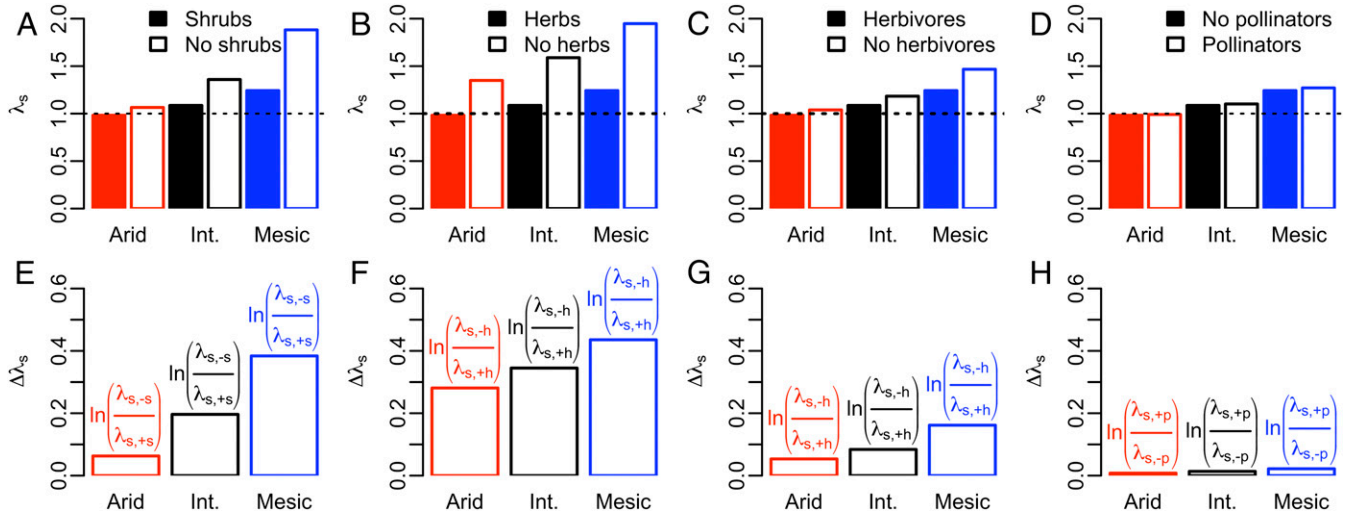

Fig. 1. Aridity and all four species interactions affected *H. meyeri* population growth rate (λ_s). We calculated λ_s with natural levels of the species interactions (filled bars) and with modified levels of the species interactions (open bars) at each site (*A–D*) and calculated the mean log ratio of each λ_s pair ($\Delta\lambda_s$; *E–H*) across 1,000 replicates incorporating model and parameter uncertainty. For antagonistic interactions, we estimated effects on λ_s using the ratio of growth in the absence of the interaction (indicated by −s and −h) to that under natural levels of the interaction (*A–C* and *E–G*, indicated by +s and +h); for simulated pollinators, to preserve the same scaling, we used the opposite ratio (*D* and *H*; +p indicates the presence of simulated pollinators, and −p indicates the absence of simulated pollinators). Int., Intermediate site.

S1), but the much higher Mesic site fruit-to-seedling transition rate means that the effects of shrubs on reproductive rates generated much larger increases in λ_s at the Mesic than Arid site. For herbivores, aridity-driven differences in reproduction (combined probabilities of fruiting and number of fruits among plants that fruited) directly generated the majority of the SIASH pattern (Fig. 4*C*, Fig. S2, and Table S1), although survival and mean growth also contributed (and fruit-to-seedling transition rate countered the net effect). In sum, at the Mesic site, the life history of *H. meyeri* was altered such that λ_s was far more sensitive to the effects of all four species interactions on vital rates, especially those that altered reproduction or recruitment (Fig. S4).

Discussion

Population growth of *H. meyeri* was more sensitive to species interactions in abiotically less stressful areas, supporting the fundamental pattern hypothesized by SIASH (8). This finding accords with prior experimental and correlative studies, including Connell's (12, 13) experimental studies on predation and herbivory in intertidal ecosystems and work describing broad-scale patterns in species distributions (14, 17, 19, 21, 24, 25). Our findings of weaker net competitive effects of herbs and shrubs in the Arid site are also consistent with the predictions of the stress gradient hypothesis (22), although we do not see evidence of net facilitative effects on population growth under any conditions in our study.

Variation in plant life history across the aridity gradient was integral to generating the SIASH pattern: aridity sharply decreased fruit-to-seedling transition rate, which in turn reduced the sensitivity of population growth to both this vital rate itself, as well as, less substantially, to other vital rates associated with offspring production (Fig. S4). Low sensitivities to these vital rates in the Arid site resulted in weak population-level effects of species interactions that affected offspring production. This finding differs from the common assumption that the SIASH pattern arises due to higher densities or diversities of interacting species in less stressful areas (5, 7, 25). This life history mechanism could generate the SIASH pattern in many systems and should operate whenever (*i*) one or more proportional sensitivities to λ_s decrease with stress and (*ii*) species interactions have similar proportional effects on vital rates across a stress gradient. One other full demographic study provides evidence that the proportional sensitivity of λ to vital rates might differ systematically across environmental gradients in just this way (32). However, we also note that the life history mechanism could also generate the opposite of the SIASH pattern if proportional sensitivities to λ_s increase with stress.

The strong effects of aridity on vital rate sensitivities associated with offspring production and survival that we see here seem likely to be present for many plant populations that occur across stress gradients. Stress, specifically aridity, tends to have the strongest negative impacts on younger and more vulnerable life stages, such that seed establishment and seedling survival are strongly impacted (33–36). These negative impacts will tend to decrease the relative effect of species interactions that affect offspring production on population growth, leading to the exact SIASH pattern we document here.

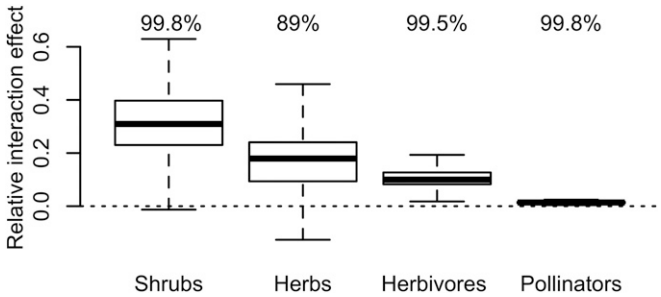

Fig. 2. Species interactions exerted stronger effects on λ_s in less stressful areas. The difference between Mesic and Arid $\Delta\lambda_s$ (Fig. 1) represents the relative interaction effect (RIE), with RIE > 0 indicating stronger effects of manipulating species interactions at the Mesic site than the Arid site. Boxplots show predictions incorporating model and parameter uncertainty, and numbers above boxes indicate the percentage of 1,000 replicates where RIE > 0. For antagonistic interactions, we estimated effects on λ_s using the ratio of λ_s with a species interaction removed to that with the natural levels of the species interaction; for simulated pollinators, to preserve the same scaling, we used the opposite ratio.

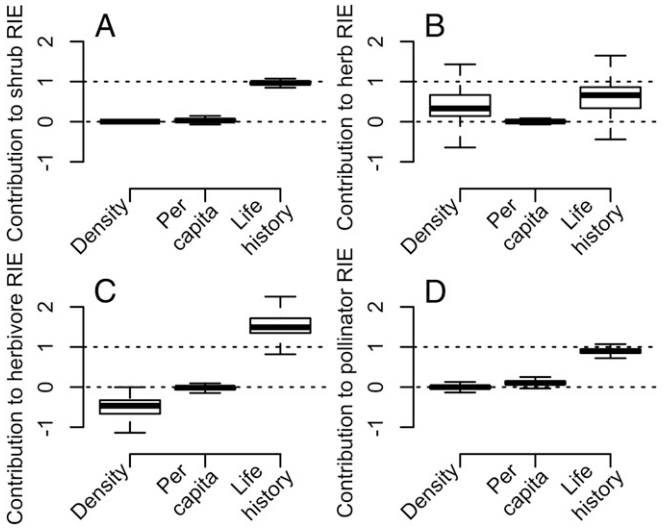

Fig. 3. The SIASH pattern arose primarily from the life history mechanism. Boxplots show RIE values, incorporating model and parameter uncertainty of 1,000 replicates, decomposing the mechanisms creating greater effects of species interactions on λ_s in the Mesic vs. Arid site, for shrubs (*A*), herbs (*B*), herbivores (*C*), and simulated pollinators (*D*). Values are standardized by dividing by the total RIE from a replicate, so that with strict additivity the three values would sum to 1. Positive numbers indicate that the mechanism contributed to the expected SIASH pattern; negative numbers indicate mechanisms opposing the net pattern (e.g., the density mechanism for herbivory, *C*, contributed to stronger effects of herbivores in the Arid site, opposing the net SIASH pattern).

In our study, per capita effects of species interactions and density of interactors were largely unchanged with stress (Fig. S2). In other species or other species interactions, per capita effects on vital rates might differ with stress, such that we would not see the same level of support for SIASH that we observe in this study. For example, antagonistic interactions such as herbivory, predation, or parasitism might exert negligible effects on vital rates in less stressful areas because individuals are better able to compensate for damage (37) or deter attack (38, 39), resulting in weaker support for SIASH. Alternatively, if interactor density decreases with stress, then we might see stronger support for SIASH, as well as stronger effects of the density mechanism in generating the SIASH pattern (as we found for effects of herbs on *H. meyeri*). The density mechanism might play a crucial role over larger spatial scales, such as latitudinal gradients, that can exhibit strong variation in interactor diversity and density (40). Although our results were consistent across a multitude of species interactions and suggested a strong role for the life history mechanism, further demonstrating the generality of the pattern will require attention to a broader range of taxa and stress gradients. In the case of multiple uncorrelated abiotic stressors, support for SIASH will depend on patterns of interactor density and diversity, per capita impacts of interactors, and life history of the focal organism across the combined stress gradients; the latter two in particular are poorly understood for most species, even across a single axis of one type of stress.

Our results suggest that species interactions may be the strongest force setting *H. meyeri* range boundaries in less stressful areas by limiting population growth and ultimately driving $\lambda_s < 1$. We did not see direct evidence for population decline due to species interactions, likely because our experiment was not near the species' mesic range boundary; while precipitation in our experiment spans an appreciable fraction (8%) of the range of annual precipitation levels experienced by *H. meyeri* across its range, the conditions at our study sites were on the arid end of the species' climate envelope (*Supporting Information*). For species interactions to set the mesic range boundary would require that impacts of species interactions on population growth continue to increase with rainfall and offset any positive, direct effects of increasing moisture. Confirmation of this hypothesis would require transplant experiments beyond the species' climatic range boundaries combined with manipulations of species interactions, as well as tests of other potential range boundary drivers.

Collectively, our data show that the effects of species interactions on population growth rate vary as a function of stress, a crucial step in distinguishing abiotic vs. biotic controls of both population growth and range boundaries. Consistent with the apparent lack of abiotic control over some warm-edge range boundaries (19, 24), our results suggest that species interactions could constrain many trailing edge boundaries (24) while having relatively weak effects on leading edge boundaries. Furthermore, we show that this pattern results from a hitherto-largely overlooked mechanism, changes in the sensitivity patterns of population growth with decreasing stress. These results caution against ignoring or minimizing effects of species interactions when predicting future distributions (4, 41–46).

Materials and Methods

We worked at the Mpala Conservancy in central Kenya, a semiarid acacia savanna (0°17′N, 37°52′E), with little spatial temperature variation and a diverse assemblage of large mammalian herbivores (*Supporting Information*). We used a replicated large-scale exclusion experiment arrayed across a pronounced rainfall gradient [Ungulate Herbivory Under Rainfall Uncertainty (UHURU) (28)] to manipulate mammalian herbivores. UHURU comprises 36 1-ha plots, including unfenced controls and three size-selective exclosure treatments; each treatment is replicated three times in blocks at each of three sites across the rainfall gradient (Fig. S1). Total average rainfall increases 22% from the Arid to Mesic site, and soil characteristics do not vary

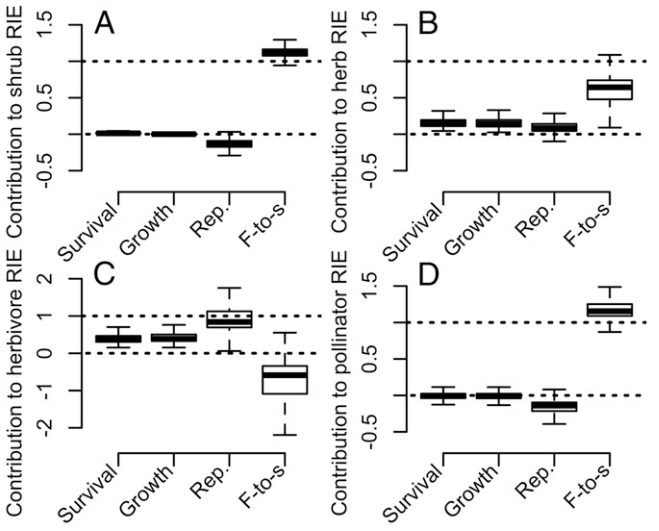

Fig. 4. The difference between fruit-to-seedling transition rate between Arid and Mesic sites was the primary vital rate difference generating the SIASH pattern. Boxplots show contributions of each vital rate to total RIE value for 1,000 replicates incorporating model and parameter uncertainty of decompositions of the vital rates, analogous to Fig. 3, for shrubs (*A*), herbs (*B*), herbivores (*C*), and simulated pollinators (*D*). Values are standardized by dividing by the total RIE from a replicate, so that with strict additivity the four values would sum to 1. Positive numbers indicate that aridity-driven differences in a vital rate contributed to the expected SIASH pattern; negative numbers indicate effects opposing the net pattern [e.g., for herbivores (*C*), fruit-to-seedling transition rate contributed to stronger effects of herbivores in the Arid site, opposing the SIASH pattern]. Note difference in scale in *D*. F-to-s, fruit-to-seedling transition rate; Rep., reproduction (probability of fruiting and number of fruits given fruiting).

substantially across this gradient (28). We used rain gauges to measure precipitation and quarterly herbivore dung counts (28) as a proxy for herbivore density (*Supporting Information*). We collected data from all herbivore exclosure treatments and used it to parameterize vital rate models, but our herbivore presence/absence contrast compares results from unfenced plots and the total-exclosure treatment, which reduces densities of all large mammal herbivores to zero.

In this ecosystem, *H. meyeri* is a common water-limited subshrub (*Supporting Information*). It is heavily browsed by multiple mammal species, has no pronounced chemical or physical defenses, and exhibits moderate compensatory regrowth following herbivory (27). Its flowers present their styles for outcross pollination by insects but can also self-pollinate if no insects visit. Self-pollination is very common, but bouts of outcrossing also occur (*Supporting Information*). *H. meyeri* life history varies substantially across this gradient (time required by the population to increase by a factor of R_0, generation time, is 22.1 y in the Arid, 15.0 in the Intermediate, and 9.9 in the Mesic site; Fig. S2).

Data Collection. In July 2011, to assess effects of rainfall and herbivory on *H. meyeri* vital rates, we searched randomly selected areas in all UHURU sites and treatments (controlling for plant phenology; ref. 27), as well as four transects outside of the UHURU experiment (two at the Mesic and two at the Arid site, each coded as a separate block for analysis), and marked and mapped all *H. meyeri* individuals, measuring size, counting fruits, and estimating percent ground cover of all vegetation in a 30-cm radius (sample sizes in Table S2). Until 2014, we returned annually to remeasure these plants, also recording survival and distance to nearest woody or succulent shrub (acacia, *Vachellia* spp., and *Senegalia* spp., as well as *Euphorbia nyikae*, *Croton dichogamous*, *Grewia* spp., *Balanities* spp., or *Boscia* sp.) >30 cm tall. Throughout the study, we marked new plants in the same areas to replace dead individuals for a total of 1,719 unique individuals followed.

To quantify the effect of herbaceous neighbors on plant vital rates, we marked and measured haphazardly chosen plants (arrayed across the size spectrum) in the total-exclosure and unfenced control plots and transects at all sites (26), randomly assigned one-third to a neighbor removal treatment, and removed all herbaceous biomass within a 30-cm radius, carefully painting the cut stalks with herbicide (glyphosate) to prevent resprouting. We repeated this biomass removal procedure twice yearly and remeasured all plants annually, replacing dead or missing plants as necessary, for a total of 1,504 individuals (Table S2).

Unlike the experimental approach used for herbs and herbivores (which estimates the effect of experimentally reducing species interactions from their naturally occurring densities to zero) and the observational approach we used for shrubs (which quantifies the effect of shrubs at naturally occurring average vs. far distances), we used a simulation-based approach based on partial observational data to estimate the possible effects of pollinators. We used work on a congeneric species with a similar floral phenotype [*Hibiscus trionum* (29); *Supporting Information*] to simulate a release from inbreeding depression caused by increased pollinator visitation rate (which affected two vital rates, fruit-to-seedling transition rate and number of fruits given fruiting). Our pollinator simulations assume that all fruits we observed in the field were self-pollinated, and represent a shift from 0% outcross pollination to 100% outcross pollination (both plausible outcomes, as field observations indicated that per-plant outcross-pollination rates were usually either 0% or 100%; *Supporting Information*). Thus, our results reflect the maximum possible effect pollinators could exert in this system (but see *Supporting Information*), although we do not experimentally quantify their effect.

We obtained fruit-to-seedling transition rate data by counting all seedlings in a 2-m radius around fecund individuals arrayed across all site*exclosure-treatment combinations immediately after a wet season.

Statistical Analysis. We used corrected Akaike information criterion (AICc) to select best-fit mixed-effects models for survival, mean growth, variance in growth, probability of fruiting, number of fruits produced, and fruit-to-seedling transition rate. We identified the best models from all subsets of a global model with initial biomass and all two-way interactions between rainfall (measured as site- and year-specific rainfall totals), herbivore activity (estimated via dung counts in each herbivore exclosure treatment*block combination), neighboring herbaceous plant cover, and distance to nearest shrub as fixed effects (or all interactions among rainfall, herbivore activity, and neighboring biomass cover as fixed effects for fruit-to-seedling transition rate; *Supporting Information*). Using continuous predictor variables (e.g., dung counts rather than herbivore exclosure treatment, or rainfall rather than site) allowed us to capitalize on spatiotemporal variation in these predictor variables to improve our predictions of vital rate responses.

For each of the three sites, we constructed stochastic IPMs (31) for each of five kernels representing different combinations of species interactions: (*i*) field conditions: + herbs, + shrubs, + herbivores, − simulated pollinators; (*ii*) field conditions − shrubs; (*iii*) field conditions − herbs; (*iv*) field conditions − herbivores; (*v*) field conditions + simulated pollinators, using 5 y of rainfall data (*Supporting Information*).

We incorporated both model and parameter uncertainty into our estimates of λ_s values (and hence effects of species interactions on λ_s). To do so, for each vital rate, we first selected a model from among those with ΔAICc $\leq$ 2 and with a probability of selection proportional to the model's AICc weight, and then sampled from the multivariate distribution of fixed-effect parameter estimates for the selected model (Table S1) and calculated each of the five above kernels for each set of parameter values. We replicated this procedure 1,000 times. For each replicate and species interaction, we calculated $\Delta\lambda_s = \ln(\lambda_s$ with altered species interactions$/\lambda_s$ under field conditions) for both Mesic ($\Delta\lambda_{s,M}$) and Arid ($\Delta\lambda_{s,A}$) sites to obtain an RIE value (RIE $= \Delta\lambda_{s,M} - \Delta\lambda_{s,A}$). We present a graphical illustration of our approach to calculate $\Delta\lambda_s$ in Fig. 1 and our approach to calculate RIE in Fig. S3. Effects of species interactions in the Intermediate site always fell between those at Mesic and Arid sites. Alternative methods of parameterizing IPMs yielded similar results (*Supporting Information*), and λ_s values were near unity (Fig. S5).

To understand how the density, per capita impact, and life history mechanisms contributed to the patterns of RIE values, we decomposed the change in λ_s in Mesic vs. Arid sites attributable to each. For each species interaction, we estimated three modified RIEs; for each, we set two of the following three effects to mean values (mean pooled across Arid and Mesic sites) in our mixed-model vital rate functions, leaving site-specific values for Arid and Mesic vital rate functions for only one of the three effects: (*i*) density of focal interactors (e.g., herbivore activity level); (*ii*) rainfall terms in rainfall*focal species interaction terms (e.g., rainfall*herbivore activity level); (*iii*) block effects and rainfall in all other terms besides rainfall*focal species interaction terms. Retaining site-specific terms for (*i*) represents variation in interactor density with rainfall (density mechanism), (*ii*) represents variation in per capita vital rates (per capita impact mechanism), and (*iii*) represents the variation in life history effects (life history mechanism), assuming that block effects are entirely composed of effects of rainfall differences across sites (our results are robust to this assumption; *Supporting Information*). Field densities of pollinators do not vary between the Mesic vs. Arid site; thus, we could not vary (*i*) for simulated pollinators, and the rainfall terms in rainfall*focal species interaction (*ii*) comprises all rainfall terms in fruits per plant and fruit-to-seedling transition rate, the two vital rates affected by inbreeding depression. Block effects and rainfall values in all other vital rates comprise the life history mechanism. For example, to determine herbivore RIE attributable to the life history mechanism, we set Arid and Mesic site herbivore activity level equal to the mean herbivore activity level in Arid and Mesic sites (*i*) and did the same for rainfall values in rainfall*herbivore activity terms (*ii*), such that vital rate functions for Mesic vs. Arid sites differed only in block effects and rainfall values in other terms. To obtain a modified RIE, we followed the procedure described above, but using the modified vital rate functions just described. To quantify the contribution of each mechanism, we calculated a modified RIE and compared it to an unmodified RIE that used site-specific focal species interaction levels, rainfall values, and block effects.

To assess how aridity-driven differences in each type of vital rate contributed to RIE values, we used a similar approach. In these calculations, λ_s values were generated using site-specific values of the focal species interaction on all vital rates, but only the focal vital rate had site-specific rainfall and block effects. Values for all nonfocal species interactions, as well as rainfall and block values for nonfocal vital rates, were set to mean values across both sites. Note that variance in growth was always set to mean values. In this way, we isolated the effect of rainfall (assuming that block effects were driven by rainfall) and each focal species interaction on each focal vital rate, and then used the resulting λ_s values to calculate RIE. Comparing these modified RIE values to the unmodified RIE for an interaction gives the fractional contribution of each vital rate to the total RIE.

All data used to construct IPM projections are archived on figshare.

ACKNOWLEDGMENTS. We acknowledge funding from the Philanthropic Educational Organization Scholar Award; United Nations Educational, Scientific and Cultural Organization-L'Oréal International Fellowship; Wyoming National Aeronautics and Space Administration Space Grant; funds from the Universities of Colorado and Wyoming; National Science Foundation (NSF) Division of Environmental Biology (DEB) Grant 1311394 (with D.F.D.) (to A.M.L.); NSF Awards DEB-1355122, DEB-1457691, and IOS-1656527 (to R.M.P.); NSF DEB Early Concept Grants for Exploratory Research Grant 1547679, NSF DEB Grant

1556728, and awards from the University of Wyoming and the University of Wyoming Biodiversity Institute (to J.R.G.); NSF DEB Grant 1149980 (to T.M.P.); NSF DEB Grant 1242355 (to W.F.M. and D.F.D.); Strategic Environmental Research and Development Program Grant 15 RC01-096 (to W.F.M.); and NSF DEB Grant 1352781 (to D.F.D.). The UHURU experiment was built with a Natural Sciences and Engineering Council Research Tools and Instruments grant.

1. Gaston KJ (2003) *The Structure and Dynamics of Geographic Ranges* (Oxford Univ Press, New York).
2. Sexton JP, McIntyre PJ, Angert AL, Rice KJ (2009) Evolution and ecology of species range limits. *Annu Rev Ecol Evol Syst* 40:415–436.
3. Parmesan C (2006) Ecological and evolutionary responses to recent climate change. *Annu Rev Ecol Evol Syst* 37:637–669.
4. Alexander JM, Diez JM, Hart SP, Levine JM (2016) When climate reshuffles competitors: A call for experimental macroecology. *Trends Ecol Evol* 31:831–841.
5. Darwin C (1859) *On the Origin of Species by Means of Natural Selection* (J. Murray, London).
6. Dobzhansky T (1950) Evolution in the tropics. *Am Sci* 38:209–221.
7. MacArthur RH (1972) *Geographical Ecology: Patterns in the Distribution of Species* (Harper and Row, Princeton).
8. Louthan AM, Doak DF, Angert AL (2015) Where and when do species interactions set range limits? *Trends Ecol Evol* 30:780–792.
9. Brooker R, et al. (2005) The importance of importance. *Oikos* 109:63–70.
10. Miller TEX, Louda SM, Rose KA, Eckherg JO (2009) Impacts of insect herbivory on cactus population dynamics: Experimental demography across an environmental gradient. *Ecol Monogr* 79:155–172.
11. Matassa CM, Trussell GC (2015) Effects of predation risk across a latitudinal temperature gradient. *Oecologia* 177:775–784.
12. Connell JH (1961) Effects of competition, predation by *Thais lapillus*, and other factors on natural populations of the barnacle *Balanus balanoides*. *Ecol Monogr* 31:61–104.
13. Connell JH (1961) The influence of interspecific competition and other factors on the distribution of the barnacle *Chthamalus stellatus*. *Ecology* 42:710–723.
14. Newsome TM, et al. (2017) Top predators constrain mesopredator distributions. *Nat Commun* 8:15469.
15. Fourcade Y, Öckinger E (2016) Host plant density and patch isolation drive occupancy and abundance at a butterfly's northern range margin. *Ecol Evol* 7:331–345.
16. Gutierrez D, Vila R, Wilson RJ (2016) Asymmetric constraints on limits to species range influence consumer-resource richness over an environmental gradient. *Glob Ecol Biogeogr* 25:1477–1488.
17. Peers MJL, Thornton DH, Murray DL (2013) Evidence for large-scale effects of competition: Niche displacement in Canada lynx and bobcat. *Proc Biol Sci* 280:20132495.
18. Sanford E, Roth MS, Johns GC, Wares JP, Somero GN (2003) Local selection and latitudinal variation in a marine predator-prey interaction. *Science* 300:1135–1137.
19. Ettinger AK, Ford KR, HilleRisLambers J (2011) Climate determines upper, but not lower, altitudinal range limits of Pacific Northwest conifers. *Ecology* 92:1323–1331.
20. Jankowski JE, Robinson SK, Levey DJ (2010) Squeezed at the top: Interspecific aggression may constrain elevational ranges in tropical birds. *Ecology* 91:1877–1884.
21. Pasch B, Bolker BM, Phelps SM (2013) Interspecific dominance via vocal interactions mediates altitudinal zonation in neotropical singing mice. *Am Nat* 182:E161–E173.
22. Brooker RW, Callaghan TV (1998) The balance between positive and negative plant interactions and its relationship to environmental gradients: A model. *Oikos* 81: 196–207.
23. Godsoe W, et al. (2016) Interspecific interactions and range limits: Contrasts among interaction types. *Theor Ecol* 10:167–179.
24. Sunday JM, Bates AE, Dulvy NK (2012) Thermal tolerance and the global redistribution of animals. *Nat Clim Chang* 2:686–690.
25. Hargreaves AL, Samis KE, Eckert CG (2014) Are species' range limits simply niche limits writ large? A review of transplant experiments beyond the range. *Am Nat* 183: 157–173.
26. Louthan AM, Doak DF, Goheen JR, Palmer TM, Pringle RM (2014) Mechanisms of plant-plant interactions: Concealment from herbivores is more important than abiotic-stress mediation in an African savannah. *Proc Biol Sci* 281:20132647.
27. Louthan AM, Doak DF, Goheen JR, Palmer TM, Pringle RM (2013) Climatic stress mediates the impacts of herbivory on plant population structure and components of individual fitness. *J Ecol* 101:1074–1083.
28. Goheen JR, et al. (2013) Piecewise disassembly of a large-herbivore community across a rainfall gradient: The UHURU experiment. *PLoS One* 8:e55192.
29. Seed L, Vaughton G, Ramsey M (2006) Delayed autonomous selfing and inbreeding depression in the Australian annual *Hibiscus trionum* var. *vesicarius* (Malvaceae). *Aust J Bot* 54:27–34.
30. Ruiz-Guajardo JC (2008) Community plant–pollinator interactions in a Kenyan savannah. PhD dissertation (University of Edinburgh, Edinburgh).
31. Ellner SP, Childs DZ, Rees M (2016) *Data-Driven Modelling of Structured Populations* (Springer, Berlin).
32. Angert AL (2006) Demography of central and marginal populations of monkeyflowers (*Mimulus cardinalis* and *M. lewisii*). *Ecology* 87:2014–2025.
33. Moles AT, Westoby M (2004) Seedling survival and seed size: A synthesis of the literature. *J Ecol* 92:372–383.
34. Evans MEK, Ferrière R, Kane MJ, Venable DL (2007) Bet hedging via seed banking in desert evening primroses (*Oenothera,* Onagraceae): Demographic evidence from natural populations. *Am Nat* 169:184–194.
35. McDowell N, et al. (2008) Mechanisms of plant survival and mortality during drought: Why do some plants survive while others succumb to drought? *New Phytol* 178: 719–739.
36. Eckhart VM, et al. (2011) The geography of demography: Long-term demographic studies and species distribution models reveal a species border limited by adaptation. *Am Nat* 178(Suppl 1):S26–S43.
37. Maschinski J, Whitham TG (1989) The continuum of plant responses to herbivory: The influence of plant association, nutrient availability, and timing. *Am Nat* 134:1–19.
38. Nelson RJ, Demas GE (1996) Seasonal changes in immune function. *Q Rev Biol* 71: 511–548.
39. Wirsing AJ, Steury TD, Murray DL (2002) Relationship between body condition and vulnerability to predation in red squirrels and snowshoe hares. *J Mammal* 83:707–715.
40. Schemske DW, Mittelbach GG, Cornell HV, Sobel JM, Roy K (2009) Is there a latitudinal gradient in the importance of biotic interactions? *Annu Rev Ecol Evol Syst* 40:245–269.
41. Afkhami ME, McIntyre PJ, Strauss SY (2014) Mutualist-mediated effects on species' range limits across large geographic scales. *Ecol Lett* 17:1265–1273.
42. Tingley R, Vallinoto M, Sequeira F, Kearney MR (2014) Realized niche shift during a global biological invasion. *Proc Natl Acad Sci USA* 111:10233–10238.
43. Van der Putten WH, Macel M, Visser ME (2010) Predicting species distribution and abundance responses to climate change: Why it is essential to include biotic interactions across trophic levels. *Philos Trans R Soc Lond B Biol Sci* 365:2025–2034.
44. Blois JL, Zarnetske PL, Fitzpatrick MC, Finnegan S (2013) Climate change and the past, present, and future of biotic interactions. *Science* 341:499–504.
45. Raffa KF, Powell EN, Townsend PA (2013) Temperature-driven range expansion of an irruptive insect heightened by weakly coevolved plant defenses. *Proc Natl Acad Sci USA* 110:2193–2198.
46. Araújo MB, Luoto M (2007) The importance of biotic interactions for modelling species distributions under climate change. *Glob Ecol Biogeogr* 16:743–753.
47. Armbruster P, Reed DH (2005) Inbreeding depression in benign and stressful environments. *Heredity (Edinb)* 95:235–242.
48. Sandner TM, Matthies D (2016) The effects of stress intensity and stress type on inbreeding depression in *Silene vulgaris*. *Evolution* 70:1225–1238.
49. Polhill D (1988) *Flora of Tropical East Africa: Index of Collecting Localities* (Royal Botanic Gardens, Kew, UK).
50. Hijmans R, van Etten J (2016) Raster: Geographic Data Analysis and Modeling. R Package, Version 2.5-8. Available at https://CRAN.R-project.org/package=raster. Accessed March 17, 2017.
51. Wang HH, et al. (2015) Species distribution modelling for conservation of an endangered endemic orchid. *AoB Plants* 7:plv039.
52. Hijmans RJ, Cameron SE, Parra JL, Jones PG, Jarvis A (2005) Very high resolution interpolated climate surfaces for global land areas. *Int J Climatol* 25:1965–1978.
53. Caylor K, Gitonga J, Martins D (2016) *Mpala Research Center Meteorological and Hydrological Dataset* (Mpala Research Center, Laikipia, Kenya).

Supporting Information

Louthan et al. 10.1073/pnas.1708436115

Results of Predictions Using Alternate Models and Response Variables

Analogous values for predictions using global models (models that include all two-way interactions shown in Table S1) for $\Delta\lambda_s$ values from Fig. 1 in the main text are as follows: − shrubs: Arid: −0.24 (SD, ±0.4514); Intermediate: 0.182 (0.4182); Mesic: 0.544 (0.2809); −herbs: 0.215 (0.1852), 0.293 (0.1886), 0.377 (0.1771); − herbivores: 0.033 (0.0332), 0.056 (0.0382), 0.123 (0.0347); + simulated pollinators: 0.01 (0.0043), 0.016 (0.0053), 0.023 (0.0054). Note that, for shrubs, we see strong support for the stress gradient hypothesis when using global models: larger facilitative effects than competitive effects in the Arid site and larger competitive effects than facilitative effects in the Mesic site (22). The Mesic site effects are stronger than Arid site effects, supporting SIASH. See Fig. S6 for an analogous figure that includes only per capita effects of species interactions and results using only best-fit models. Support for SIASH is robust to different numbers of mesh points, and to analyzing differences or ratios of λ_s values. Finally, the values of RIE used in Figs. 3 and 4 (− shrubs: mean: 0.3555, SD: 0.1386; − herbs: 0.0895, 0.1126; − herbivores: 0.0487, 0.0308; and + simulated pollinators: 0.0154, 0.0039) were calculated when setting non-focal interacting species densities to the mean value (mean across Mesic and Arid sites) and also show support for SIASH. Note that these RIE values differ from values of RIE shown in Fig. 2: Fig. 2 RIEs were calculated using site-specific predictor variables for all interactions.

When calculating the contributions of our three mechanisms to RIE, we included site-specific block effects in the life history mechanism. This inclusion assumes that block effects in our mixed models arise entirely from rainfall effects on vital rates. However, in addition to differences in rainfall among sites and blocks, block effects could also include unmeasured variables that differ across sites (e.g., insect herbivory, unmeasured soil characteristics, etc.). To ensure that support for the life history mechanism is driven primarily by a vital rate response to rainfall rather than these unmeasured variables, we recalculated RIE contributions of each mechanism while maintaining site-specific block effects in all vital rates. For all species interactions besides herbs, the life history mechanism remains the primary driver of stronger effects of species interactions in the Mesic than Arid site. For herbs, the per capita mechanism becomes the primary driver, with life history a secondary driver. Thus, our results are largely robust to assuming that block effects are only driven by unmeasured differences across sites, rather than at least partly driven by differences in rainfall across sites.

Further Details on Estimating the Effects of Simulated Pollinators on λ_s

***Hibiscus meyeri* Pollination Syndrome.** *H. meyeri* has a floral phenotype that appears to favor outcrossing by an insect vector but presumably assures self-fertilization in the absence of an effective pollination event. Similar to a well-studied *Hibiscus* in this same system (30), *H. meyeri* displays flowers for only 1 d; stigmas remain exposed to outcross pollen until the afternoon, when, if they have not received outcross pollen, they bend back to touch their style to the anthers surrounding the style (resulting in self-pollination). *Hibiscus trionum*, a facultative selfer with a similar floral phenotype to *H. meyeri*, shows weak, delayed inbreeding depression, likely due to repeated incidences of self-fertilization (29). In *H. trionum*, performance of selfers compared with outcrosses was worst for maternal seeds per fruit (outcross to selfer performance ratio = 1.0526) and flowers per plant in the F_1 generation (ratio = 1.0989) (29).

Simulation Approach to Estimate Effects of Pollination on Populations. We opportunistically collected data on the fraction of self-pollinated flowers in 245 plants across all sites and herbivore exclosure treatments from 2010 to 2013. On a per-plant basis, the fraction of self-pollinated flowers in the field ranges from 0 to 1, but there is little variation among sites in average selfing rate (Arid site = 0.99, Intermediate = 0.99, Mesic = 1.0); note that incorporating lower selfing rates in Arid sites into our analysis would result in even weaker effects of simulated pollinators in Arid sites.

Most commonly, plants self-pollinate all their flowers, but some plants receive outcross pollen on all their flowers (80% of plants had ≥90% of flowers selfed, 13% of plants had ≤10% selfed, where "selfed" is defined as flowers on which a style recurved more than 90° when surveyed between 2 and 4 PM). Thus, we assumed that all observed *H. meyeri* plants selfed in the field, and for our pollination treatment, we simulated outcrossing of all flowers by adding a fractional increase of 1.0526 in fruit-to-seedling transition rate (which includes seeds per fruit) and a fractional increase in 1.0989 in number of fruits given fruiting (which includes flowers per plant); effects on seeds per fruit and flowers per plant are the two strongest effects of inbreeding depression in *H. trionum* (29). Thus, our pollinator treatment represents the most optimistic gains possible in pollinator service: complete selfing to complete outcrossing, but these are both realistic possibilities in the field. Note that our results showing support for SIASH for simulated pollinators are likely to largely arise from one simple life history effect; Mesic site population growth rate was much more sensitive than Arid site population growth rate to one of the vital rates that simulated pollinators affect, fruit-to-seedling transition rate.

Inbreeding Depression May Vary with Stress. There is some evidence that effects of inbreeding depression may be more severe in stressful environments (47). Thus, a change from 0 to 100% outcross pollination may have more substantial impacts in our Arid site than in the Mesic site. When incorporating a 69% increase in the magnitude of inbreeding depression in the Arid site compared with the Mesic site [species-wide average of increase in inbreeding depression in stressful vs. less stressful locations, according to a recent review (47)], we see stronger effects of simulated pollinators in the Arid site, completely contrary to SIASH. We did not incorporate this 69% increase in inbreeding depression in Arid sites in *H. meyeri* for three reasons: (*i*) while some of the "benign" locations in this review were greenhouse conditions, watering *H. meyeri* in the Mesic site still increases performance, indicating the Mesic site is clearly still stressful; (*ii*) lineages within an inbred population often exhibit very different relationships between stress and inbreeding depression, suggesting inconsistent responses across genotypes (47); and (*iii*) 24% of species show no change at all in inbreeding depression with stress (47). In fact, a recent paper showed the opposite trend (inbreeding depression decreased with stress) for multiple stressors (including aridity) (48).

Further Details on Model Fitting and Integral Projection Matrix Construction

All analyses were conducted in R, version 3.3.2. Before fitting the models, we first ensured that inclusion of each subset of our data (unmanipulated plants, unmanipulated haphazardly selected plants,

and unmanipulated plants within and outside of the UHURU experiment) did not unduly change the parameter estimates of the global model. For fruit-to-seedling transition rates, we counted seedlings in a 2-m radius around 35 fruiting plants after a wet season. While we tried to obtain a larger sample size, sample size is low due to missing data. However, we see good support for our best-fit models; cumulative AICc weight is 0.518 (Table S1). Critically, for all three best-fit models, average block effect in the Mesic site is larger than average block effect in the Arid site (block effects drive higher fruit-to-seedling transition rate in the Mesic site; Table S1). To fit models, we used ln(seedling number/fruit number) as a response variable. Block and observer (of initial plant size) were random effects in all vital rate models besides fruit-to-seedling transition. Fruit-to-seedling transition had only block as a random effect (all of the measurements were done by the same observer). Note that our estimates of fruit production and fruit-to-seedling transition rates are based on discrete measurements during one time period. While we conducted these measurements in the wet season at the height of reproduction and germination, fruit and seedling production is erratic across time; thus, we may be underestimating total seedling production and thus population growth.

We conducted replicate measurements by different observers at the same time (or within 32 h) to estimate observer effects on our measurement of size. Our two metrics of size, basal area and height, were strongly correlated across multiple observers. A.M.L. performed measurements consistently throughout the duration of this study. Average fractional deviation from A.M.L.'s measurements [(alternate observer's measurements − A.M.L.'s measurements)/A.M.L.'s measurements] was small (0.14 for basal area and 0.12 for height), and the R^2 of log-transformed basal area × height (we use basal area × height in our biomass estimation; see below) of a linear regression between the alternate observer's measurements and A.M.L.'s measurements was 0.93. Furthermore, the random effect of observer only explained a small fraction of total variance of the models for vital rates (maximum fraction of variance explained by observer across all models used was <0.051).

In our IPM, discretized kernels were constructed with 26 size classes, and seedlings entered the kernel with a height of 5.44 cm and a basal area of 0.96 mm^2, the mean of all *H. meyeri* with height <10 and a basal diameter of 2 (the upper limits for newly observed plants in the field). To generate estimates of λ_s for each combination, we initiated projections with the averaged stable size distribution (averaged across the five different years' kernels) for a given site*block, and then projected population sizes forward, sampling annual kernels with equal probability for 10,000 y. We discarded the first 2,000 y, to guard against transient dynamics, then averaged the remaining years' λ to obtain λ_s, and then averaged λ_s across each site's blocks. We discarded all model and parameter combinations that predicted ≤0 seedlings per fruit. The global model for seedlings per fruit often predicted ≤0 seedlings per fruit, so we used the best-fit model for fruit-to-seedling transition rate in our global projections, rather than the global model. Our methods are standard for both matrix models and IPMs, so could be described as being either of these very similar types of models.

When calculating RIE for the decompositions, we set nonfocal species interaction types to the mean of the Mesic and Arid site values to isolate the effect of rainfall and the focal species interaction (e.g., when assessing the effect of herbs, we set herbivore, pollinator, and shrub density to their mean value across the Arid and Mesic site); thus, total RIE for the decomposition approach is not the same as the RIE in Fig. 2. For the decomposition of vital rates, variance in growth was set to mean values.

To obtain mean matrices to get elasticities, as well as generation times, we generated kernels for each combination of site, five annual rainfall values, and block, and then averaged over rainfall years and blocks to get site-specific kernels. These kernels used field conditions for species interactions (+ herbs, + shrubs, + herbivores, − simulated pollinators) and best-fit parameter estimates of all best-fit models with ΔAICc ≤ 2, the same suite of models used in the main text (weighting the predicted vital rates with their corresponding models' AICc weight). As in our main analyses, we discarded seedlings per fruit values ≤0. We obtained elasticities via perturbation.

Estimates of Total *H. meyeri* Biomass

To generate a unified metric of size, we measured and harvested above-ground biomass of 30 plants arrayed equally across the three sites, drying to a constant weight and then regressing log-transformed dry biomass on log-transformed basal area × height. This gave us biomass = exp(0.3338488 × log(basal area × height)), which had an R^2 of 0.88.

Plants subject to neighbor removal treatments show a different relationship between basal area and height (increased basal area growth relative to height, perhaps due to alleviation of light limitation). To generate a separate biomass regression for plants subject to neighbor removal treatments, in July 2012 we also conducted neighbor removal treatments on 19 plants (7 at the Intermediate site, 3 at the Arid site, 9 at the Mesic site; sample sizes are unequal due to mortality after establishment of these treatments, and for each site, we had roughly equal numbers of plants in both herbivore total-exclosure treatments and areas open to herbivores). In June 2014, we measured and harvested these plants, drying to a constant weight and then regressing log-transformed dry biomass on log-transformed basal area × height. This gave us biomass = exp(0.3593906 × log(basal area × height)), which had an R^2 of 0.90. We used these two equations to get estimates of biomass for both unmanipulated plants and plants subject to neighbor removal treatments.

Rainfall Data and Effects of Rainfall on *H. meyeri* Performance

Rainfall Is a Stressor. We know that water is a limiting resource for *H. meyeri*. First, we observed the highest λ_s values in the Mesic site (Fig. S5). Also, we conducted a watering experiment within the herbivore total-exclosure treatment at each of the three sites, watering 19–21 plants at each site (see Table S2 for sample sizes) with 7.5 L every month for 10 mo (March 2014 to Feburary 2015) and comparing their growth to the growth of unmanipulated control plants over this same interval. This level of rainfall approximated one-half of the long-term average of rain in the Mesic site (2009–2012; we initiated a pilot watering experiment in 2012). We then compared five models of mean growth as a function of (*i*) site*watering treatment interaction; (*ii*) site + watering treatment; (*iii*) site alone; (*iv*) watering treatment alone; and (*v*) intercept only, with block as a random effect in all models. While the best-supported model indicates constant growth rates regardless of site or watering treatment (AICc weight, 0.486), the second-best–supported model indicates a positive effect of additional water on plant growth (AICc weight, 0.239), suggesting that rainfall is a stressor in the field. A greenhouse study shows no evidence for local adaptation to rainfall.

Determination of Annual Rainfall. Average annual rainfall from 2009 to 2014 is 486.4 mm/y in the Arid site, 577.4 mm/y in the Intermediate site, and 593.8 mm/y in the Mesic site (Fig. S7). Rainfall data before June 2010 come from manual rain gauges (one at each of the three sites), and after from automatic rain gauges (two to three at each of the three sites) in the herbivore total-exclosure treatments (28). Note that these rainfall amounts differ from those amounts reported in previous papers on the same *H. meyeri* system because they include rainfall data from more years than previous studies.

Calculation of Predictor Variables for Vital Rate Models and for Projections of λ_s

For all of our analyses, we collected data from all herbivore exclosure treatments and use all of these data to fit our mixed models for vital rates. When projecting population growth rate in the presence vs. absence of herbivores, we compare results from the total-exclosure treatment (which excludes all herbivores) and the completely open treatment (which lets in all herbivores).

Rainfall. We used cumulative rainfall (the average of two to three automatic rain gauges at each site) between the midpoint of the first *H. meyeri* remeasurement period (this period was usually 2–3 mo long) and the midpoint of the second *H. meyeri* remeasurement period as a predictor variable (or for 12 mo before measurement for fruit-to-seedling transition rate). Specifically, we used rainfall between each of our *H. meyeri* remeasurement periods as a predictor variable for survival, mean growth, and variance in growth during that same interval, as well as reproduction at the end of that interval.

Herbivore Activity. Similarly, we used dung counts (a proxy for herbivore activity) during the interval as a predictor of survival, mean growth, and variance in growth during that interval and reproduction at the end of that interval (or for 12 mo before measurement for fruit-to-seedling transition rate). For each dung survey*site*block*treatment combination, we summed total dung counts collected along three transects to get an estimate of herbivore activity per survey (28). To obtain an estimate of average herbivore activity in each site*block*herbivore exclosure treatment during the intervals between *H. meyeri* measurements, we averaged the quarterly counts from the dung counts conducted between the midpoint of the first *H. meyeri* remeasurement period and the midpoint of the second *H. meyeri* remeasurement period. We used the midpoint of the dates over which the dung survey was conducted as the date of the dung survey in this analysis. For our initial measurements, we averaged the data from the dung counts collected over the previous year. We discarded dung counts for hippo, which were only counted in one survey (only one dung pile was found), as well as for all carnivores. For one survey, the Intermediate site blocks 1 and 2 were not labeled, so we discarded these dung counts. For another survey, we did not count the dung of 3 species (out of 12 species), so we replaced these missing data with zeros, as average dung counts across all transects for these 3 species were 0.004, 0.004, 0.005 piles/transect, respectively.

For our transects outside of the UHURU plots, for which we had neither rainfall data nor herbivore dung counts, we used that site's rainfall value, and we used the average of all that site's blocks' herbivore dung counts for a given time period. Transects were ~200 m from the plots, and thus likely experience similar herbivore densities and rainfall levels.

Other Predictor Variables. Each plant had an associated value for percent cover (percent ground cover of vegetation in a 30-cm radius) as well as an associated distance to shrub, measured annually.

Predictor Variables Used in Projections of λ_s. For the predictor variables in our projections, presented in main text Fig. 2, we used the observed rainfall values between our *H. meyeri* remeasurement periods to get site-specific values of rainfall for each of 4 y. We averaged across all blocks' observed herbivore activity values between our *H. meyeri* remeasurement periods to get year*site*herbivore exclosure treatment-specific herbivore activity predictor variables, and then averaged across years. Average naturally occurring herbivore activity levels (in UHURU open control treatments, open to herbivores) were as follows: 23.6 (Arid), 21.5 (Intermediate), and 13.4 (Mesic).

For neighboring biomass cover, we averaged all nonmanipulated plants' observed values in each year*site*herbivore exclosure treatment to get a mean value for each site*herbivore exclosure treatment, and then averaged across years. Average naturally occurring neighboring biomass cover levels (in UHURU open control treatments, open to herbivores) were as follows: 46.0 (Arid), 43.4 (Intermediate), and 64.4 (Mesic); recall that these are percent covers. For distance to shrub, we used the median of all nonmanipulated plants' observed distances in each site*herbivore exclosure treatment, averaged across years, as the presence of the interaction, and the maximum distance ever observed in unmanipulated plants as the absence of the interaction. Median naturally occurring distances to shrub (in UHURU control treatments, open to herbivores) were as follows: 69.7 cm (Arid), 54.7 (Intermediate), and 50.2 (Mesic); maximum was 915. Note that averaging across years removes any across-year covariance between interacting species' densities and rainfall: given that our measurement of rainfall is a cumulative metric, a long-term average of interacting species' density over both rainy and dry years (similar to the breadth of rainfall experienced during wet and dry seasons), rather than a year-specific value, seemed more appropriate.

For our projections in field conditions, we used the following as predictor variables: (*i*) the site-specific open control neighboring biomass cover average value for neighboring biomass cover; (*ii*) the site-specific open control median distance to shrub for distance to shrub; (*iii*) the site-specific open control dung counts for herbivore activity; (*iv*) the predicted number of fruits given fruiting and fruit-to-seedling transition rates using field data. *Hibiscus meyeri* fruits have a maximum of 15 seeds, so we fixed the maximum seedlings per fruit at 15. For predictions without shrubs, we changed (*ii*) above to the maximum distance to shrub observed across all sites and herbivore exclosure treatments. For predictions without herbs, we changed (*i*) above to 0. For predictions without herbivores, we changed (*i*), (*ii*), and (*iii*) above to analogous herbivore total-exclosure treatment values. For predictions with simulated pollinators, (*i*), (*ii*), and (*iii*) were as for field conditions, but (*iv*), the predicted number of fruits given fruiting and fruit-to-seedling transition rate using field data, were multiplied by 1.0989 and 1.0526, respectively. For our results with nonspecific predictor variables shown in Fig. S6, we averaged across the sites to get values for these predictions.

A Theoretical Decomposition of the Factors Contributing to RIE

As defined in the text, the RIE measures the change in the impact of a species interaction on the population growth rate of a focal species along a gradient of abiotic conditions from less stressful to more stressful. SIASH proposes that antagonistic species interactions exert a more negative impact on population growth as the harshness of the abiotic environment declines. A key idea is that changes in one or more vital rates change the pattern of sensitivities of population growth to underlying vital rates, such that the same effects of interacting species on vital rates can have quite different impacts on λ if other vital rates differ.

To explain the different mechanisms that can influence RIE, in this appendix, we derive an analytical approximation for a change, $\Delta\lambda$, in the deterministic population growth rate λ as a function of changes in vital rates (e.g., survival, growth, and reproductive rates) and in sensitivities of λ to the vital rates, driven by differences in both the abiotic environment and species interactions. (Note that $\Delta\lambda$ in all that follows in this appendix is different from the $\Delta\lambda$ in the main text, as we are here following standard notation for Taylor expansions.)

We start with a simpler expression for RIE than the one used in the main text:

$$\mathrm{RIE} = \left(\lambda^{(\mathrm{WO,M})} - \lambda^{(\mathrm{W,M})}\right) - \left(\lambda^{(\mathrm{WO,A})} - \lambda^{(\mathrm{W,A})}\right), \qquad \textbf{[S1]}$$

where the superscripts indicate population growth rate without (WO) or with (W) the interacting species and in the Mesic

(M) or Arid (A) environment. We will consider $\lambda^{(WO,A)}$ as a baseline population growth rate, as it is the rate when the abiotic variable (i.e., rain) and the density of the interacting species are at low levels. We can expand the expression for RIE in [**S1**] by considering how the other three λ's change relative to the baseline $\lambda^{(WO,A)}$. For example, we could let

$$\lambda^{(W,M)} = \lambda^{(WO,A)} + \Delta\lambda(\Delta d_a, \Delta d_b), \qquad \textbf{[S2]}$$

where $\Delta\lambda(\Delta d_a, \Delta d_b)$ is the change in λ (relative to the baseline) when we change the abiotic variable (rain) by an amount Δd_a and the density of the interacting species by an amount Δd_b (where the subscript b indicates that this is the species interaction of interest). If we have a general expression for $\Delta\lambda(\Delta d_a, \Delta d_b)$, we can use it to estimate all three of the λ's (other than the baseline) in [**S1**]. The second-order Taylor expansion of λ as a function of the underlying vital rates, the v_i's, provides such a general expression:

$$\Delta\lambda \approx \sum_i \Delta v_i \frac{\partial\lambda}{\partial v_i} + \frac{1}{2}\sum_i\sum_j \Delta v_i \Delta v_j \frac{\partial^2\lambda}{\partial v_i \partial v_j}, \qquad \textbf{[S3]}$$

where the $\partial\lambda/\partial v_i$'s, the so-called sensitivities of the population growth rate to the underlying vital rates, and their higher-order derivatives are evaluated at the baseline condition and the Δv_i's are the changes in the vital rates in response to changes in abiotic conditions and species interactions.

Now we consider two of the vital rates, v_m and v_n, which contribute the following term to the right-hand side of [**S3**] (plus additional terms with cross partial derivatives involving v_m or v_n, but not both):

$$\Delta v_m \frac{\partial\lambda}{\partial v_m} + \Delta v_n \frac{\partial\lambda}{\partial v_n} + \frac{1}{2}\Delta v_m^2 \frac{\partial^2\lambda}{\partial v_m^2} + \Delta v_m \Delta v_n \frac{\partial^2\lambda}{\partial v_m \partial v_n} + \frac{1}{2}\Delta v_n^2 \frac{\partial^2\lambda}{\partial v_n^2}. \qquad \textbf{[S4]}$$

Because RIE in [**S1**] measures the change in the impact of a species interaction with a change in an abiotic factor along a gradient, each of the terms in [**S4**] will contribute to RIE only if they change with both a change in the abiotic factor and the presence of the species interaction; otherwise, these terms will contribute identical values to the difference in λ without vs. with the species interaction in Mesic and in Arid sites, and thus will cancel out in the expression for RIE in [**S1**]. Let us assume that the abiotic factor affects both vital rates, v_m and v_n, but that the species interaction affects only v_m. In particular, we assume that

$$\Delta v_m \approx \Delta d_a \frac{\partial v_m}{\partial d_a} + \Delta d_b \frac{\partial v_m}{\partial d_b} \text{ and } \Delta v_n \approx \Delta d_a \frac{\partial v_n}{\partial d_a}, \qquad \textbf{[S5]}$$

where Δd_a and Δd_b are as defined above, and the partial derivatives represent the sensitivities of these two vital rates to the abiotic and species interaction variables, and again are evaluated at the baseline condition. In this situation, the only terms in [**S4**] that contribute to the RIE are as follows:

$$\left(\Delta d_a \frac{\partial v_m}{\partial d_a} + \Delta d_b \frac{\partial v_m}{\partial d_b}\right)\frac{\partial\lambda}{\partial v_m}, \qquad \textbf{[S6]}$$

$$\frac{1}{2}\left(\Delta d_a \frac{\partial v_m}{\partial d_a} + \Delta d_b \frac{\partial v_m}{\partial d_b}\right)^2 \frac{\partial^2\lambda}{\partial v_m^2}, \qquad \textbf{[S7]}$$

$$\left(\Delta d_a \frac{\partial v_m}{\partial d_a} + \Delta d_b \frac{\partial v_m}{\partial d_b}\right)\Delta d_a \frac{\partial v_n}{\partial d_a}\frac{\partial^2\lambda}{\partial v_m \partial v_n}. \qquad \textbf{[S8]}$$

In each of these terms, Δd_b represents the effects of changing the density of the interacting species on RIE (our "density mechanism"), while $\partial v_m/\partial d_b$ represents the per capita effects of the species interaction on the vital rate that it directly affects (our "per capita impact mechanism"; specifically, it is the slope of a line describing how the vital rate changes with changing densities of the interacting species). In [**S7**], the second partial derivative $\partial^2\lambda/\partial v_m^2 = \partial/\partial v_m(\partial\lambda/\partial v_m)$ represents the change in the sensitivity of the population growth rate to v_m as the abiotic drivers and density of the interacting species changes (thus changing v_m), which is part of our "life history mechanism." That is, it represents the effect of changes in life history with changing aridity that will alter the effects of species interactions on λ. In addition, Eq. **S8** illustrates a second part of the life history mechanism: when a change in the abiotic factor drives a change in a vital rate that is not directly affected by the species interaction (such as v_n), the impact of the species interaction on the population growth rate can nevertheless change because changes in the life history cause changes in the sensitivities to other vital rates (e.g., v_m) that are affected by the species interaction (this change in sensitivity is represented by the term $\partial^2\lambda/\partial v_m \partial v_n = \partial/\partial v_n(\partial\lambda/\partial v_m)$ in [**S8**]).

Thus, in summary, RIE can be driven by (*i*) a change in the density of the interacting species along the gradient (our density mechanism); (*ii*) a change in the per capita effects of the interacting species (our per capita impact mechanism); (*iii*) a change in the life history causing changes in the sensitivities of population growth to vital rates that are affected by the species interaction; and (*iv*) a change in the sensitivity of population growth to vital rates affected by the species interaction because of changes in other vital rates not affected by the species interaction. The direct and indirect changes generated by (*iii*) and (*iv*) together comprise our life history mechanism.

Herbivore Species and Densities

Herbivore Species. Large common herbivores in UHURU include elephant (*Loxodonta africana*), giraffe (*Giraffa camelopardalis*), eland (*Taurotragus oryx*), buffalo (*Syncerus caffer*), zebra (*Equus quagga*), waterbuck (*Kobus ellipsiprymnus*), impala (*Aepyceros melampus*), warthog (*Phacochoerus africanus*), and dik-dik (*Madoqua guentheri*) (27). The mammalian herbivore community composition is similar across sites, with elephant (*Loxodonta africana*), impala (*Aepyceros melampus*), and dik-dik (*Madoqua guentheri*) dominating (28).

Densities of Herbivores Across Herbivore Exclosure Treatments and sites. Herbivore exclosure treatments are highly effective and herbivore densities are higher in our Arid site. We used dung count data from 19 dung count surveys used in this study, conducted between July 2010 and May 2015, to test for differences in herbivore activity. We summed total dung found in each site*herbivore exclosure treatment*block*survey combination, and then averaged across blocks for each survey. We found a significant effect of site on log-transformed dung counts in control areas open to herbivores [ANOVA, $F_{(2,56)} = 5.69$, $P = 0.006$], with higher herbivore activity in the Arid site than in the Mesic site [Tukey's honest significant difference (HSD), $P = 0.005$]. Mean dung count values in open controls are as follows: Arid site, 23.0; Intermediate, 19.8; and Mesic, 14.0. Herbivore exclosure treatment had significant effects on total dung: a two-way ANOVA revealed nonsignificant effects of site and site*herbivore exclosure treatment, but significant effects of herbivore exclosure treatment [$F_{(3,218)} = 94.7488$, $P < 2e\text{-}16$]. The open control treatment, open to all herbivores, had greater amounts of total dung than the total-exclosure treatment, closed to all herbivores (Tukey's HSD, $P << 0.05$).

UHURU Is Representative of a Substantial Fraction of *H. meyeri*'s Geographic Range and Is Thus Likely to Be Reflective of Dynamics at the Range Edge

We see no variation in *H. meyeri* density across this rainfall gradient in field conditions (densities calculated as in ref. 27; $P > 0.05$), and this could be for two reasons: (*i*) the extreme patchiness of its distribution means that our local estimates of density may not reflect average density differences as a function of rainfall; or (*ii*) this species is undergoing shifts in its geographic range (with the Mesic site becoming more suitable for *H. meyeri*, but density is not yet high). Shifts in *H. meyeri*'s geographic range over time would suggest that range boundaries are not stable in this species, and thus that our results on the effects of abiotic stress or species interactions must be interpreted in light of trailing vs. leading range boundaries, rather than the factors that set range boundaries. To test that *H. meyeri* range boundaries were stable, we recorded descriptions (mostly of general localities, not of specific GPS locations) of locations of *H. meyeri*, *Hibiscus callyphyllus*, and *Hibiscus micranthus* herbarium specimens at the National Museums of Kenya, and if GPS coordinates were missing, we converted these to exact locations (49). We discarded specimens whose label indicated that they were located in an artificial environment (e.g., greenhouse or garden), or that had insufficiently precise location information (>150-km-diameter range). We supplemented these locations with data from the Global Biodiversity Information Facility, using the getData() function in R's raster package (50). We assumed that all locations at which *H. meyeri* was collected were presences, but locations at which *H. callyphyllus* or *H. micranthus*, but not *H. meyeri*, were collected were absences (51) (Fig. S7). We then removed duplicates (plants collected in the same place) and constructed a simple climate envelope model: we first extracted BioClim variables (at the 2.5-min scale) (52) for locations of *H. meyeri* presence and absence, and then used a model selection approach to determine whether mean annual temperature, mean annual precipitation, and seasonality of precipitation, or some combination of these, best explained *H. meyeri* presence. Only mean annual precipitation and seasonality of precipitation were present in the best-fit model, with no effect of mean annual temperature.

We used the best available herbarium records for this work, but they suffer from at least two limitations. First, there is a clear sampling bias in our herbarium records: few specimens were collected in Mozambique or Tanzania (Fig. S7*A*). Second, the year of these collections varies widely, from 1858 to 2009, and the WorldClim dataset we used here is only representative of 1960–1990 (52). Due to these reasons, we do not show any predictions of the climate envelope model but rather show actual precipitation values of herbarium specimen locations. We note that our inference that precipitation is much more important than temperature is likely correct, as our presence/absence data span a wide temperature gradient (Fig. S7*A*).

Our model selection approach suggests that mean annual temperature does not affect *H. meyeri* occurrence, but that higher total precipitation and higher variability in precipitation reduce probability of occurrence. Supporting these results, *H. meyeri* presence records occur over a smaller range of annual precipitation than do absence records (Fig. S7*C*). *Hibiscus meyeri* presence records have a lower precipitation seasonality than do absence records (Fig. S7*D*), suggesting that seasonality of precipitation is also a critical driver of *H. meyeri* presence.

UHURU spans a substantial fraction of the variability in precipitation experienced by this species throughout its range, for both mean annual precipitation and precipitation seasonality (Fig. S7 *C* and *D*), but does not represent range boundary conditions. UHURU is substantially closer to the arid, rather than mesic, end of the range: the long-term average of mean annual rainfall at the Mesic site is near the mean annual rainfall at which most herbarium specimens of *H. meyeri* occur [although the mean annual rainfall during our experiment was lower than the long-term average (Fig. S7*C*), note there is substantial interannual variability in rainfall (Fig. S7*B*)]. The Arid site is further from the center of the range of precipitation values at which *H. meyeri* occurs but still well within "normal" conditions. Furthermore, both the Mesic and the Arid site are well within *H. meyeri*'s niche for seasonality in precipitation. Our finding of strong effects of species interactions at the Mesic site (which is near *H. meyeri*'s optimal climate conditions across its range) suggests that species interactions should strongly affect *H. meyeri* throughout most of its range, as about one-half of *H. meyeri* occurrences are at rainfall values higher than the Mesic site.

To test whether *H. meyeri*'s range is shifting with climate change, we subdivided our herbarium records by year, removed duplicates, and generated presence–absence data in the same manner as for our climate envelope model. We then asked whether there was a significant relationship between year of collection date and the climatic variable of the occupied site, but found none (although *H. meyeri* presences show a marginally significant shift to lower mean precipitation over time, bio12, $P = 0.0621$). Due to high variability among years in collecting effort, coupled with a small sample size of presence records (Fig. S8), we were unable to infer whether *H. meyeri*'s geographic range had shifted through time.

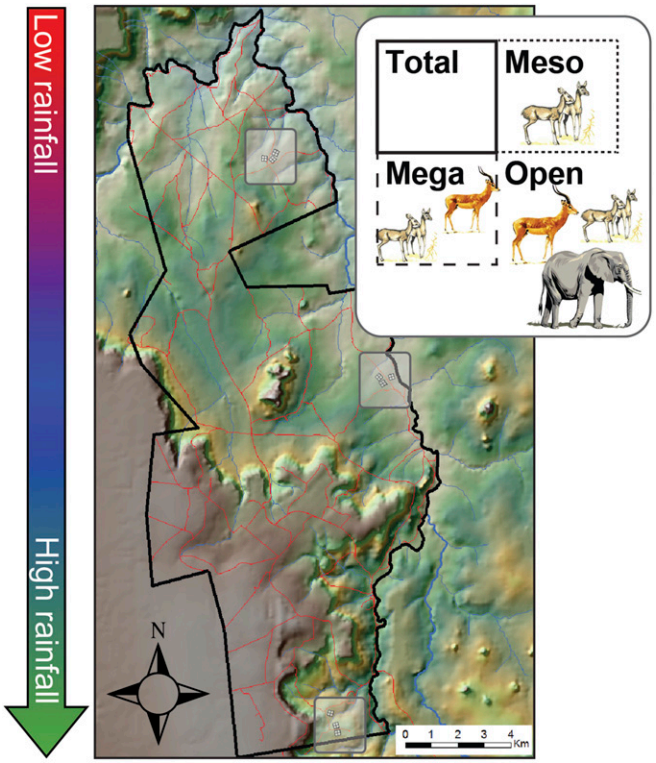

Fig. S1. Schematic of UHURU experiment. Across each of three locations (indicated by gray boxes) spanning an aridity gradient at Mpala Conservancy (outlined in black), there are three replicates ("blocks") of a set of herbivore exclosures. In our study of herbivore effects, we contrasted "Total" (no mammalian herbivore access) with "Open" (all mammalian herbivore access).

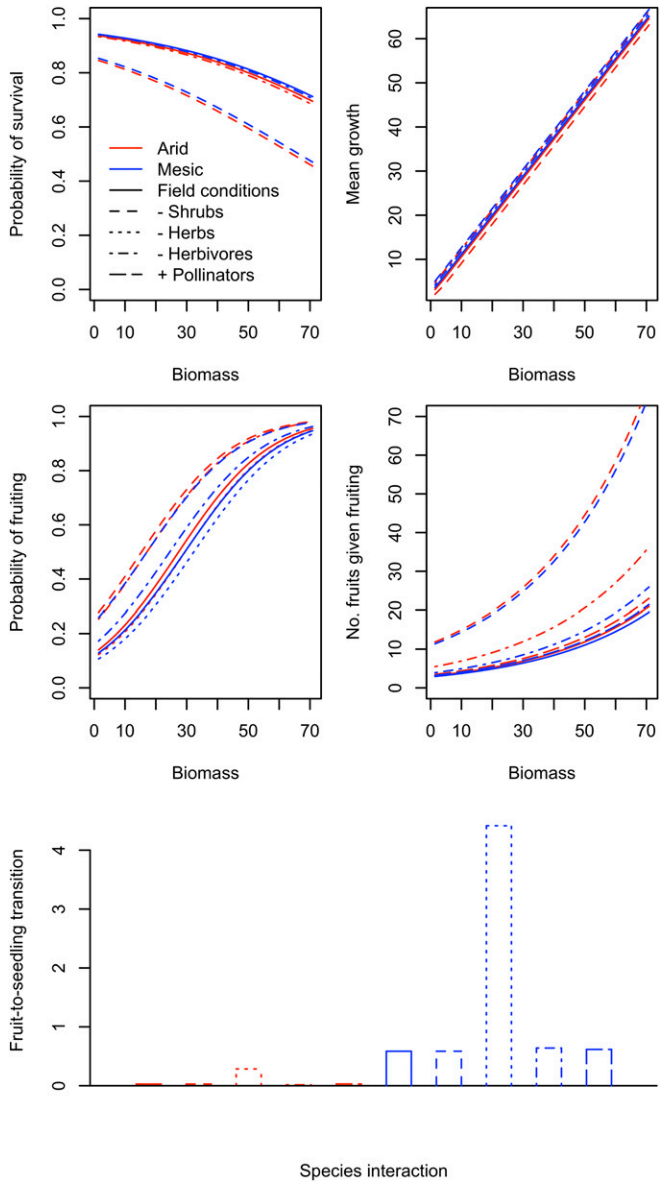

Fig. S2. Effect of aridity and species interactions on vital rate values for survival, mean growth, probability of fruiting, number of fruits given fruiting, and fruit-to-seedling transition rate. We show changes in vital rates resulting from best-fit models of species interactions. If a line is not present, vital rate does not differ from field conditions.

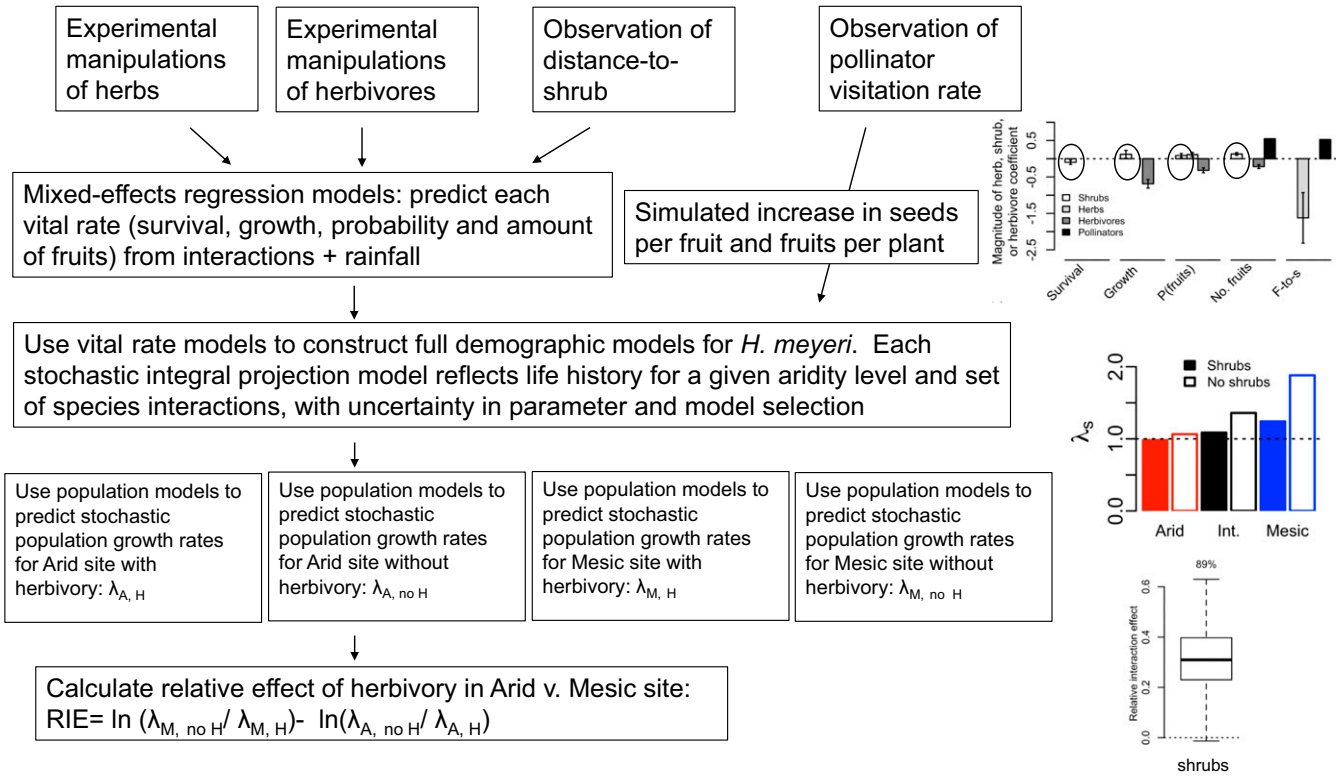

Fig. S3. Flow chart of modeling approach for RIE values. We describe how we use an integral projection model (IPM) approach to generate stochastic IPMs from mixed-effects regression models for each vital rate, incorporating both model and parameter uncertainty from the mixed-effects regression models. Here, we show an approach for shrubs, but analogous approaches apply for our three other species interactions. We generate stochastic IPMs for each aridity level (Arid, Intermediate, and Mesic) in the presence of all species interactions, as well as for each aridity level*manipulation of each species interaction (removal for herbs, herbivores, and shrubs, addition for simulated pollinators). Simulated results of manipulation of pollination is accomplished by modifying the mixed-effects regression model's predicted seeds per fruit and fruits per plant. We modify this approach to quantify each mechanisms' contribution to RIE; we use the same mixed-effect models to construct the same set of λ_s (as in this figure), but with two added steps. First, we alter the mixed-effect regression models, such that either (*i*) focal interacting species densities, (*ii*) rain terms in rain*focal interacting species terms, (*iii*) block effects/rainfall in all other terms vary across aridity levels, or none of these terms varies across aridity levels. Second, we compare RIE values from each of these modifications to an unmodified RIE that used aridity level-specific focal species interaction levels, rainfall values, and block effects, quantifying the impact of each of the three mechanisms outlined in the text on generating RIE. All *Inset* figures are replicates of figures in the main text and of Fig. S4, such that $n = 1{,}000$, error bars in the *Uppermost Inset* are SE of coefficients, and *Lowermost Inset* is a standard boxplot. F-to-s, fruit-to-seedling transition rate; Int., Intermediate site.

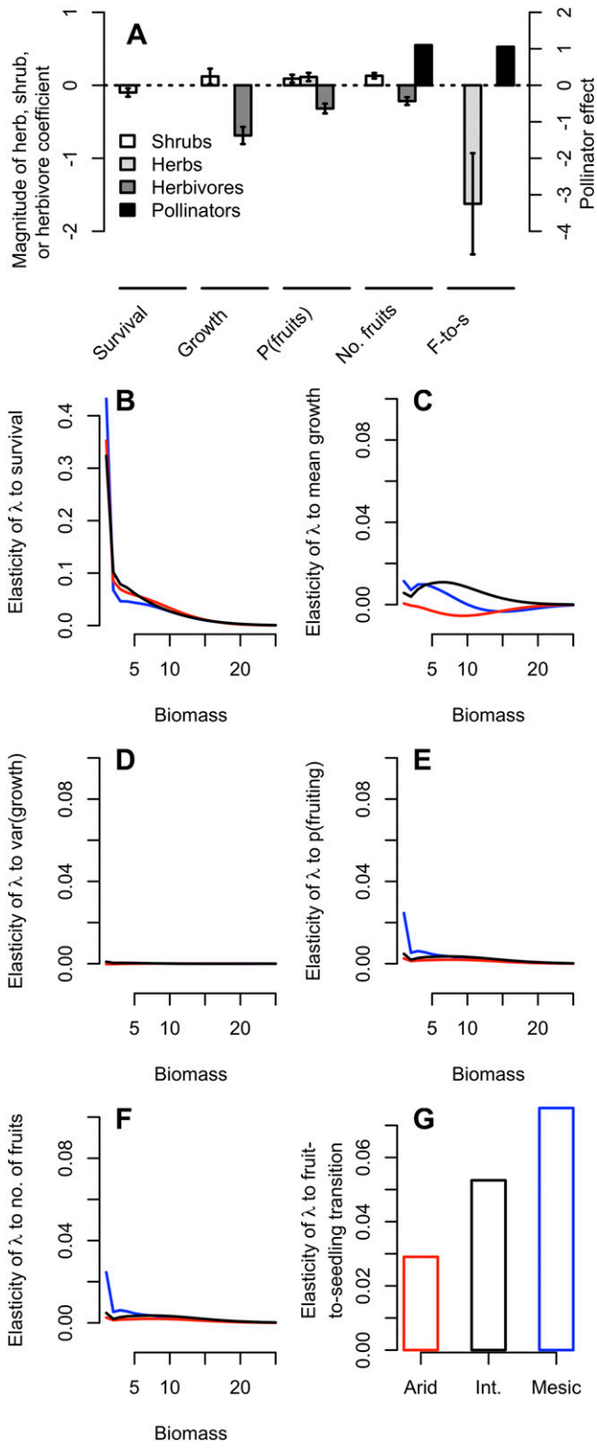

Fig. S4. The sensitivity of population growth to some vital rates is higher in the Mesic site. As is standard practice in demography, we use elasticities to show the sensitivity of population growth to changes in a vital rate, where elasticity is the estimated proportional change in population growth rate away from its baseline value with a given proportional change in the vital rate. For reference, *A* shows the sign and magnitude of best-fit fixed-effect coefficients for herbs, shrubs, and herbivores on each vital rate (for interaction and variance coefficients, see Table S1), from models fit with standardized predictor variables, so values reflect relative effect size. Absence of bars indicates that the fixed effect was not present in the best-supported model; error bars indicate SE of coefficients. The effect of simulated pollinators on vital rates is multiplicative and therefore shown on a different scale than other species interactions (*Right y* axis), and has no SE. *B*–*G* show elasticities of λ to size-specific vital rates [*B*, survival; *C*, mean growth; *D*, variance in growth; *E*, probability of fruiting; *F*, number of fruits; and *G*, fruit-to-seedling transition rates] at Arid, Intermediate, and Mesic sites. We obtained values via perturbation of kernels for each combination of site, five annual rainfall values, and block at each site, and then averaged over rainfall years and blocks to get site-specific kernels. These kernels used field conditions for species interactions (+ herbs, + shrubs, + herbivores, − simulated pollinators) and best-fit parameter estimates of all best-fit models with ΔAICc $\leq$ 2, the same suite of models used in the main text (weighting the predicted vital rates with their corresponding models' AICc weight). As in our main analyses, we discarded seedlings per fruit values $\leq$0. Note change of scale in *B*. F-to-s, fruit-to-seedling transition rate; Int., Intermediate site; no. fruits, number of fruits given fruiting per reproductive individual; p(fruits), probability of fruiting.

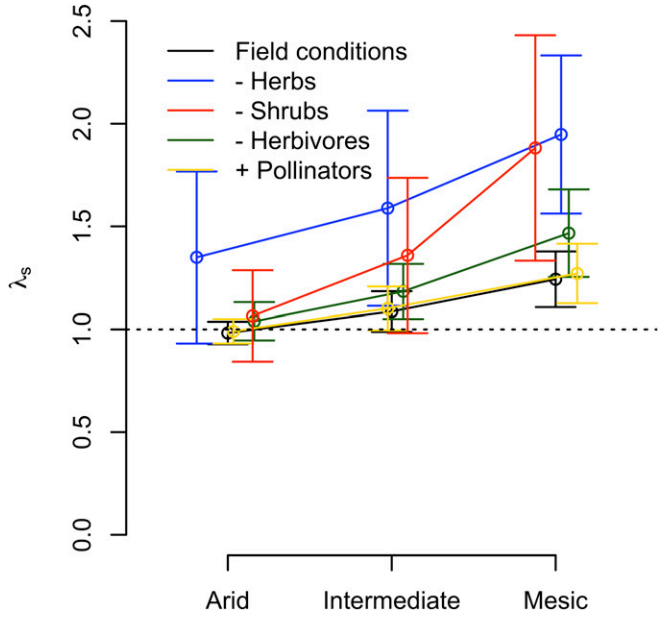

Fig. S5. λ_s as a function of aridity, in field conditions and with altered species interactions (with model and parameter uncertainty). Dotted line shows where $\lambda_s = 1$, and points are jittered for better readability. Bars represent ±SD. Note that the uncertainty in λ_s values is not fully reflected in RIE values, as the index is calculated within sets of λ_s estimates sharing both random model and parameter uncertainty.

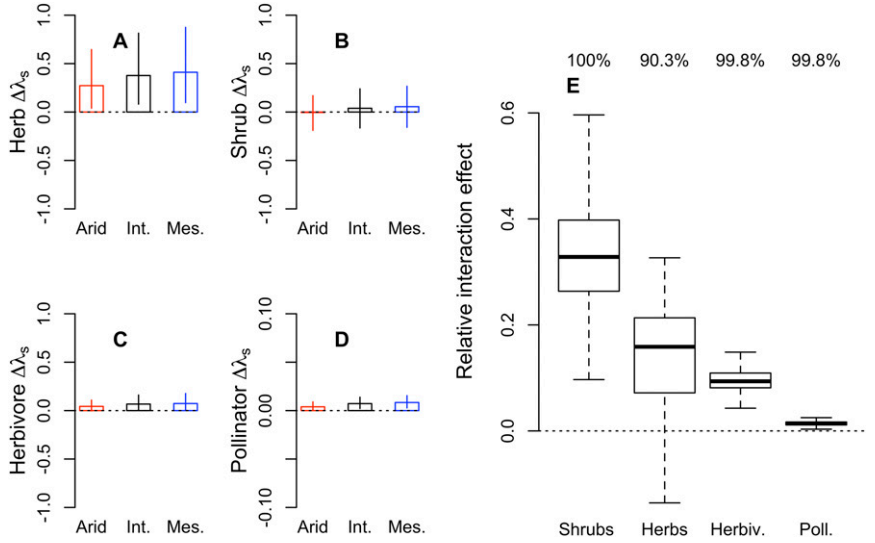

Fig. S6. SIASH is robust to alternate model formulations. *A–D* indicate change in λ_s after altering species interactions with nonspecific predictor variables, across the corresponding herbivore exclosure treatment in Arid, Intermediate, and Mesic sites and no block effects. Numbers <0 indicate altering the interaction(s) reduced fitness and numbers >0 indicate altering the interaction(s) increased fitness. Differences [ln(λ_s with altered interaction/λ_s under field conditions)] are averaged across 1,000 replications that incorporate model and parameter uncertainty. Bars represent 10–90% CIs; note the change in scale in *D*. Note that the similarity between this figure and Fig. 1 suggest that density exerts minimal effects on the overall magnitude of the change in λ_s between Mesic and Arid sites, as our main-text analyses also indicate (besides in the case of herbs). *E* is a standard boxplot of RIE values generated using 1,000 replicates of the predictions of only best-fit models, analogous to Fig. 2. Int., Intermediate site; Mes., Mesic site.

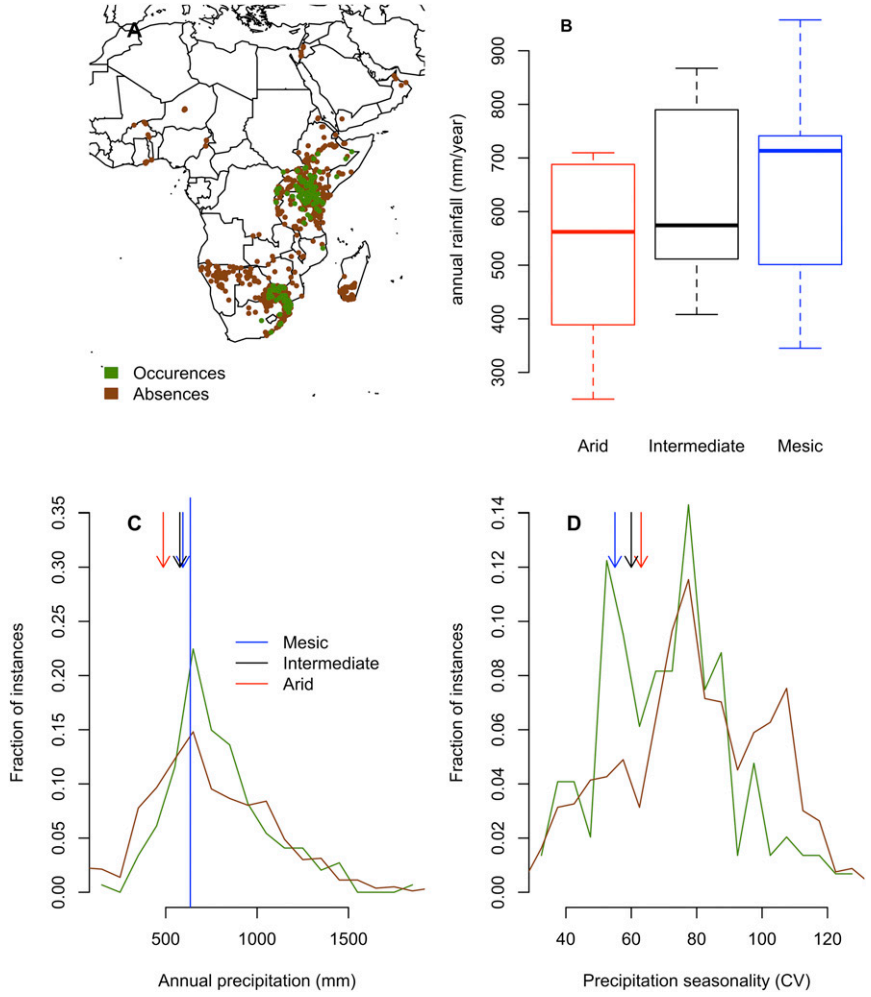

Fig. S7. Climatic niche of *H. meyeri*. *A* shows locations of known occurrences and absences of *H. meyeri* from herbarium specimen locations: note the dearth of records in Mozambique and Tanzania. *B* shows standard boxplots of annual rainfall at each site in the years used in this study. *C* shows a histogram (normalized to 1) of the mean annual precipitation of these known occurrences and absences of *H. meyeri* taken from the WorldClim dataset (Bioclim variable "Bio12") (52). Arrows indicate mean annual precipitation at the three sites in UHURU, from data taken from 2009 to 2014. Vertical bar indicates longer-term annual rainfall (1998–2015) taken at Mpala Research Centre, available only at the Mesic site (~2 km from the UHURU Mesic site) (53). *D* shows a histogram (normalized to 1) of the seasonality of precipitation of these known occurrences and absences of *H. meyeri* taken from the WorldClim dataset (Bioclim variable "Bio15") (52). Arrows indicate the WorldClim predictions of seasonality in precipitation for the UHURU sites. Direct estimates of seasonality in precipitation using rainfall data collected in UHURU yields unrealistically high estimates (Mesic, 164; Intermediate, 180; Arid, 175), likely due to an averaging effect at the low spatial resolution of WorldClim data. Estimates of seasonal variability from 1998 to 2015 at the Mesic site were not available.

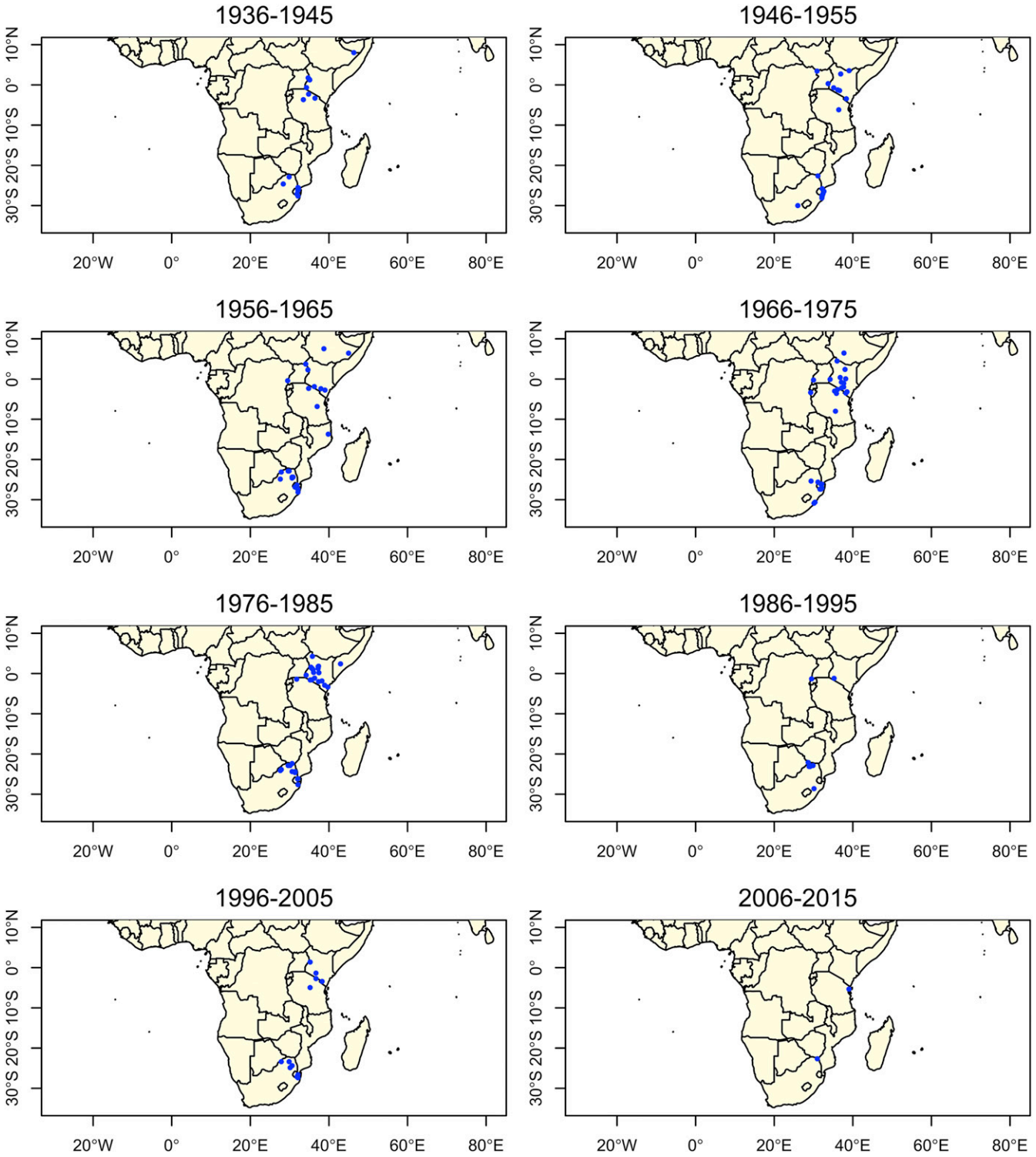

Fig. S8. Shifts in *H. meyeri*'s geographic range over time. Blue dots show locations of presence data of *H. meyeri* over 10-y increments. We see no strong evidence for a shift in *H. meyeri*'s geographic niche, although the small number of records, particularly in 1996–2015, make inference difficult.

Table S1. Fixed-effect parameter estimates for survival, growth, p(fruiting), number of fruits|fruiting occurred, and fruit-to-seedling transition

			Fixed effects													Random effects		
Vital rate	ΔAICc	AICc weight	Intercept	Initial biomass	Rainfall	Herbivore activity	Distance to shrub	Neighboring biomass cover	Rainfall*herbivore activity	Rainfall*distance to shrub	Rainfall*neighboring biomass cover	Herbivore activity*distance to shrub	Herbivore activity*neighboring biomass cover	Distance to shrub*neighboring biomass cover	Rainfall*neighboring biomass cover*herbivore activity (fruit-to-seedling transition only)	Block (SD)	Observer (SD)	Residual (SD)
			Best-fit models															
Survival	0	0.126	2.387 (0.172)	−0.268 (0.064)			−0.099 (0.056)									0.1883	0.2317	
Survival	0.74	0.087	2.387 (0.171)	−0.279 (0.063)												0.1990	0.2273	
Survival	1.33	0.065	2.389 (0.028)	−0.262 (0.064)	0.102 (0.122)		−0.100 (0.058)									0.1898	0.2202	
Survival	1.76	0.052	2.379 (0.171)	−0.274 (0.065)		−0.038 (0.076)	−0.1024 (0.058)									0.174	0.233	
Survival	1.99	0.047	2.385 (0.173)	−0.267 (0.064)			−0.100 (0.058)	0.010 (0.075)								0.190	0.234	
Mean growth	0	0.090	0.755 (0.290)	−1.115 (0.100)		−0.688 (0.117)	0.121 (0.106)		0.223 (0.147)			−0.281 (0.104)				0.908	0.143	4.225
Mean growth	0.27	0.079	0.767 (0.297)	−1.111 (0.100)	2.717 (0.157)	−0.716 (0.116)	0.116 (0.106)					−0.288 (0.104)				0.932	0.152	4.227
Mean growth	0.53	0.069	0.770 (0.293)	−1.116 (0.100)	2.795 (0.168)	−0.706 (0.118)	0.065 (0.113)	−0.080 (0.109)	0.225 (0.147)			−0.252 (0.105)	0.161 (0.097)			0.899	0.162	4.223
Mean growth	0.83	0.060	0.787 (0.302)	−1.111 (0.100)	2.772 (0.168)	−0.736 (0.117)	0.064 (0.113)	−0.093 (0.109)				−0.260 (0.105)		0.154 (0.097)		0.923	0.175	4.223
Mean growth	1.26	0.048	0.781 (0.299)	−1.111 (0.100)	2.802 (0.170)	−0.705 (0.119)	0.129 (0.106)	−0.096 (0.108)	0.213 (0.147)			−0.279 (0.104)				0.908	0.179	4.224
Mean growth	1.33	0.046	0.796 (0.306)	−1.107 (0.100)	2.78 (0.170)	−0.734 (0.117)	0.125 (0.106)					−0.285 (0.104)				0.931	0.189	4.225
Mean growth	1.37	0.045	0.784 (0.301)	−1.111 (0.100)	2.77 (0.167)	−0.739 (0.117)	0.019 (0.118)	−0.089 (0.108)		−0.173 (0.142)		−0.248 (0.105)		0.213 (0.108)		0.931	0.162	4.223
Mean growth	1.40	0.045	0.769 (0.294)	−1.115 (0.100)	2.791 (0.166)	−0.71 (0.119)	0.026 (0.118)	−0.078 (0.109)	0.209 (0.148)	−0.153 (0.143)		−0.242 (0.105)		0.213 (0.108)		0.908	0.151	4.221
Mean growth	1.98	0.033	0.755 (0.290)	−1.115 (0.100)	2.746 (0.157)	−0.688 (0.117)	0.118 (0.107)		0.219 (0.148)	−0.025 (0.128)		−0.281 (0.104)				0.91	0.141	4.225
Probability of fruiting	0	0.078	−0.887 (0.173)	0.758 (0.061)	0.813 (0.082)	−0.318 (0.067)	0.091 (0.054)	0.114 (0.057)								0.573	0	NA
Probability of fruiting	0.77	0.053	−0.89 (0.173)	0.757 (0.061)	0.813 (0.082)	−0.316 (0.067)	0.06 (0.061)	0.113 (0.057)				−0.067 (0.06)				0.576	0	NA
Probability of fruiting	0.90	0.049	−0.895 (0.179)	0.76 (0.061)	0.82 (0.081)	−0.334 (0.067)		0.121 (0.056)								0.597	0	NA
Probability of fruiting	1.40	0.039	−0.886 (0.172)	0.755 (0.061)	0.812 (0.082)	−0.319 (0.067)	0.093 (0.054)	0.114 (0.057)		0.057 (0.072)						0.572	0	NA
Probability of fruiting	1.70	0.033	−0.89 (0.172)	0.758 (0.061)	0.813 (0.082)	−0.322 (0.068)	0.092 (0.054)	0.122 (0.059)					0.033 (0.058)			0.569	0	NA
Probability of fruiting	1.85	0.031	−0.889 (0.172)	0.756 (0.061)	0.812 (0.082)	−0.318 (0.067)	0.079 (0.061)	0.115 (0.057)						0.022 (0.054)		5.72E-01	1.91E-08	NA
Probability of fruiting	1.91	0.030	−0.892 (0.173)	0.757 (0.061)	0.809 (0.083)	−0.32 (0.067)	0.091 (0.054)	0.111 (0.057)			0.027 (0.081)					5.75E-01	8.26E-08	NA
Probability of fruiting	1.86	0.029	−0.889 (0.172)	0.757 (0.061)	0.817 (0.083)	−0.318 (0.067)	0.091 (0.054)	0.114 (0.057)	0.02 (0.081)							0.572	0	NA
Probability of fruiting	1.98	0.029	−0.889 (0.173)	0.754 (0.061)	0.814 (0.082)	−0.318 (0.067)	0.059 (0.062)	0.113 (0.057)		0.067 (0.074)		−0.073 (0.062)				0.576	0	NA
No. of fruits given fruiting	0	0.099	1.513 (0.117)	0.269 (0.054)	0.488 (0.064)	−0.216 (0.053)	0.130 (0.038)									3.70E-01	1.02E-06	NA
No. of fruits given fruiting	0.96	0.061	1.514 (0.118)	0.265 (0.054)	0.486 (0.064)	−0.227 (0.054)	0.148 (0.042)					0.041 (0.039)				0.377	0.00E+00	NA
No. of fruits given fruiting	1.27	0.053	1.506 (0.116)	0.273 (0.054)	0.5 (0.067)	−0.233 (0.054)	0.133 (0.038)	0.01 (0.048)					0.076 (0.046)			0.362	0.00E+00	NA
No. of fruits given fruiting	1.67	0.043	1.505 (0.117)	0.271 (0.054)	0.506 (0.070)	−0.226 (0.055)	0.129 (0.038)		0.042 (0.067)							3.68E-01	6.63E-08	NA
No. of fruits given fruiting	1.88	0.039	1.513 (0.117)	0.269 (0.054)	0.485 (0.064)	−0.217 (0.053)	0.127 (0.038)			0.022 (0.051)						0.370	0.00E+00	NA
No. of fruits given fruiting	1.92	0.038	1.52 (0.118)	0.269 (0.054)	0.494 (0.066)	−0.216 (0.053)	0.132 (0.038)	−0.017 (0.045)								0.368	0.00E+00	NA
Seedlings per fruit	0	0.251	−0.594 (1.574)					−0.049 (0.021)								2.744	NA	2.309
Seedlings per fruit	0.74	0.154	0.519 (1.73)			−0.073 (0.054)		−0.061 (0.022)								2.616	NA	2.264
Seedlings per fruit	1.33	0.112	−1.046 (1.953)			0.118 (0.132)		−0.036 (0.027)					−0.004 (0.003)			2.730	NA	2.153
			Global models															
Survival	NA	NA	2.398 (0.16)	−0.267 (0.065)	0.12 (0.131)	−0.057 (0.08)	−0.142 (0.075)	0.009 (0.081)	−0.051 (0.106)	0.015 (0.086)	−0.081 (0.115)	−0.064 (0.065)	0.121 (0.077)	0.019 (0.067)		0.174	0.204	NA
Mean growth	NA	NA	0.759 (0.294)	−1.118 (0.1)	2.768 (0.171)	−0.699 (0.121)	0.028 (0.119)	−0.082 (0.112)	0.237 (0.157)	−0.153 (0.143)	0.065 (0.159)	−0.238 (0.106)	−0.052 (0.122)	0.21 (0.109)		0.910	0.130	4.22
Variance in growth	NA	NA	44.096 (7.409)	17.122 (1.530)	33.412 (3.077)	−0.417 (1.866)	3.409 (1.811)	−4.874 (1.720)	−14.123 (2.401)	9.271 (2.170)	−7.307 (2.436)	−5.269 (1.614)	−1.174 (1.869)	−0.683 (1.652)		18.572	8.519	64.144
Probability of fruiting	NA	NA	−0.897 (0.173)	0.753 (0.061)	0.815 (0.085)	−0.323 (0.068)	0.057 (0.069)	0.122 (0.06)	0.019 (0.083)	0.067 (0.08)	0.015 (0.083)	−0.077 (0.062)	0.038 (0.061)	0.005 (0.06)		0.571	0	NA
No. of fruits given fruiting	NA	NA	1.502 (0.118)	0.273 (0.054)	0.503 (0.073)	−0.244 (0.057)	0.175 (0.051)	0.019 (0.053)	0.036 (0.07)	0.056 (0.058)	−0.006 (0.072)	0.04 (0.041)	0.07 (0.047)	−0.056 (0.041)		0.364	0	NA

Each fixed-effects' SE is shown in parentheses, as well as SD of random effects, for both best-fit models with ΔAICc ≤ 2, and global models. AICc weights are for each vital rate individually (survival is compared against survival, for example). We fit models for variance separately for each mean growth model because all of the growth models have different residuals; while we do show the global model for variance in growth, for brevity, we do not show the best-fit variance model results because each of the nine growth models has ∼10 best-fit variance models. We fit survival and probability of fruiting with a binomial error term, mean growth and variance in growth with a normal, and number of fruits|fruiting occurred with a negative binomial (which was a better fit than a Poisson for both best-fit and global models, according to a log-likelihood test). Note that binomial and negative binomial models [survival, p(fruiting), and number of fruits|fruiting occurred] have fixed residual variance, so we do not show these values. Predictor variables are scaled for all of the vital rates besides fruit-to-seedling transition, and fruit to seedling has no observer random effect (as plants were measured by only one person). We do not show the global model for fruit-to-seedling transition, as it often predicted unrealistic values, and we did not use this model in our global predictions. Note that, to obtain coefficients used in Figs. S3 and S4, we refit the best-fit model shown in this table using standardized predictor variables. NA, missing data.

Table S2. Initial sample sizes (number of individual *H. meyeri* marked and followed) for data collection in 2011 in each site*herbivore exclosure treatment combination

Site	Herbivore exclosure treatment	Unmanipulated nonexperimental plants	Unmanipulated experimental plants	Experimental plants subject to neighbor removals	Plants subject to additional water
Intermediate	Open control	53	134	69	NA
Intermediate	Total exclosure	49	30	27	19
Intermediate	Mega	44	NA	NA	NA
Intermediate	Meso	31	NA	NA	NA
Mesic	Open control	86	161	80	NA
Mesic	Total exclosure	102	33	24	21
Mesic	Mega	88	NA	NA	NA
Mesic	Meso	68	NA	NA	NA
Arid	Open control	83	150	79	NA
Arid	Total exclosure	68	60	24	20
Arid	Mega	74	NA	NA	NA
Arid	Meso	70	NA	NA	NA
Mesic	Open transects	49	35	22	NA
Arid	Open transects	37	44	22	NA

Open controls are open to all herbivores, total exclosure excludes all herbivores larger than hares, Mega excludes mega-herbivores and larger, and Meso excludes meso-herbivores and larger. At each census, we replaced plants as necessary to maintain consistent sample sizes; plants were lost due to mortality or inability to relocate plants. For our experimental work, we tagged more plants in open-control plots than we did in total-exclosure treatment plots (due to a desire to leave some plants in total-exclosure treatments unmanipulated for future experiments). Furthermore, in total-exclosure plots, experimental plants were one-third control, one-third neighbor removal, and one-third supplemental water, while in control plots, experimental plants were one-third neighbor removal plants and two-thirds control, with no supplemental watering (a pilot experiment indicated that elephants preferentially consume supplementally watered plants, so we did not conduct this experiment in the open control). NA, missing data.